Geophysical Investigation of Cañon de Valle

Los Alamos
NATIONAL LABORATORY
— EST.1943 —

Prepared by the Environmental Programs Directorate
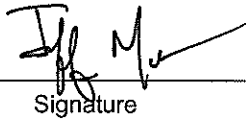
Geophysical Investigation of Cañon de Valle

July 2014

Responsible project manager:

John McCann		Project Manager	Environmental Programs	*1-25-2014*
Printed Name	Signature	Title	Organization	Date

Responsible LANS representative:

Jeff Mousseau		Associate Director	Environmental Programs	*7/29/14*
Printed Name	Signature	Title	Organization	Date

Responsible DOE representative:

Peter Maggiore		Assistant Manager	DOE-NA-LA	*7-31-2014*
Printed Name	Signature	Title	Organization	Date

TABLE OF CONTENTS

Figures

Appendixes

1.0   INTRODUCTION

This report documents the acquisition, processing, and interpretation of a direct-current (DC) electrical resistivity geophysical survey completed for Technical Area 16 (TA-16) in upper Cañon de Valle (CdV) at Los Alamos National Laboratory (LANL or the Laboratory) in Los Alamos, New Mexico (Figure 1.0-1). These field activities and this report satisfy the New Mexico Environment Department– (NMED-) approved "Work Plan for Direct Current Resistivity Profiling in Cañon de Valle" and the NMED-approved extension requests (LANL 2012, 215111; NMED 2012, 520404; NMED 2013, 523814; LANL 2014, 256573). This report also supports the corrective measures evaluation for Consolidated Unit 16-021(c)-99, the 260 Outfall, by providing information to constrain conceptual models about the hydrogeology of TA-16 (LANL 2012, 215111).

The CdV electrical resistivity investigation included acquiring, modeling (in both two- and three-dimensions), and interpreting six lines of electrical resistivity within and next to CdV at the Laboratory (Figure 1.0-2). Three lines were run parallel to the canyon and were over 5000 ft in length. The remaining three lines were placed perpendicular to the canyon to help tie the features together. Additionally, three of the resistivity lines (Lines 3, 4, and 5) had accompanying induced-polarization (IP) measurements to test chargeability effects of the different lithological units. The IP was not part of the original scope but was added during the investigation to enhance understanding of the subsurface. HydroGeophysics, Inc. (HGI) conducted this survey in May and June of 2014. Appendix A provides a detailed description of the methods and results for this survey. Appendix B presents electrical resistivity survey data.

The main objective of this study was to map the electrical structure of the vadose zone in the vicinity of CdV (LANL 2012, 215111). Of particular interest was the identification of low resistivity regions indicative of increased moisture content, clay-rich zones associated with groundwater pathways, changes in geologic lithologies, or perched water. The primary goals included the following:

- Assess the relative importance of surface water infiltration below mesa tops versus canyon floors

- Evaluate CdV as an important infiltration pathway and determine the eastern extent of infiltration

- Determine if deep perched groundwater is likely to be found north of CdV based on the deep electrical structure of the vadose zone

- Identify other low resistivity features that may be indicative of groundwater pathways (e.g., vertical infiltration zones and faults) or perching horizons (e.g., bedding)

- Evaluate the location of a new deep-perched zone monitoring well CdV-9-1(i) proposed north of CdV (LANL 2012, 213573; NMED 2013, 522693)

2.0   BACKGROUND

The 260 Outfall is the primary contaminant source with high explosive (HE) potential to impact groundwater at TA-16 (Figure 1.0-1). It received large quantities of contaminants, particularly RDX (hexahydro-1,3,5-trinitro-1,3,5-triazine), at high concentrations and large volumes of water that provided a significant hydrologic driving force for infiltration of contaminants (LANL 2011, 207069; LANL 2012, 213573). Much of the contamination released from the 260 Outfall was transported to CdV by surface-water flow. Based on the extent of perennial surface water and alluvial groundwater, the main infiltration pathway for contaminated water in CdV is located downcanyon of the 260 Outfall and extends east to the vicinity of Material Disposal Area (MDA) P, (Reid et al. 2005, 093660). Infiltration of surface water and alluvial groundwater into bedrock units results in the vertical transport of contaminants into the bedrock

units of the vadose zone. Transport of contaminants to these deeper zones is generally limited to soluble constituents such as RDX, other HE components, boron, and other organic compounds (LANL 2011, 207069).

Water percolation into bedrock is assumed to be greater beneath the canyon floors than on the mesa tops because surface flow and alluvial groundwater provide hydrologic drivers for infiltration. However, mesas have local areas of increased infiltration where sufficient hydrologic drivers exist, such as beneath ponds (e.g., the 260 Outfall pond) or beneath tributary drainages that flow during snowmelt and storm events or that received effluent in the past (LANL 2011, 207069; LANL 2012, 213573). The relative importance of these infiltration pathways was assessed by comparing DC resistivity profiles for mesa tops and canyon bottoms.

The two deep-perched groundwater zones beneath middle CdV near well R-25 are the most important in terms of contaminant pathways and are possible sources of contaminated recharge to the regional aquifer (LANL 2011, 207069; LANL 2012, 213573). Existing wells penetrating these deep-perched groundwater zones are either located in CdV or on the mesa south of the canyon (Figure 1.0-2). Because of local recharge along CdV, deep perched groundwater may be distributed symmetrically about the axis of the canyon. Consequently, contaminated deep-perched groundwater may extend north of CdV and is a potential secondary source for increasing RDX concentrations detected in the regional aquifer at well R 18 (LANL 2011, 207069).

Regional groundwater moves generally eastward in the vicinity of TA-16. At the study area, groundwater is in the Puye Formation at a depth of approximately 1200–1300 ft (LANL 2011, 207069). Figure 1.0-3 shows the potentiometric surface directly beneath the site. The regional water table is below the depth of investigation of the DC resistivity profiles and is not discussed further.

3.0   SUMMARY OF RESULTS AND CONCLUSIONS

This section provides a brief summary of the results for the DC electrical resistivity geophysical survey. A detailed description of the methods and results for this survey are in Appendix A. Preliminary interpretations of the geophysical results provided in this report will be periodically reevaluated or expanded as new subsurface data become available from deep wells planned for the area. For example, data from the planned wells R-47 and CdV-9-1(i) may provide constraints on the electrical structure of the vadose zone and lead to additional processing of the upper CdV geophysical data collected to date.

Many of the most prominent low resistivity anomalies found in this survey are associated with infrastructure such as buried utilities, power lines, and deep stainless-steel wells. These anomalies and efforts to filter out their effects are discussed more fully in Appendix A, section A-2.2.

The vadose zone exhibits a layered electrical structure. Electrical stratification of the vadose zone is best observed in lines 1 and 4 that are least affected by infrastructure effects (e.g., see Appendix A, Figures A-4.1-12 and A-4.1-13). Alluvium and weathered Qbt 4 of the Tshirege Member are conductive. This surface conductivity layer is relatively thin and has a horizontal structure. The high conductivity is likely partly the result of the presence of unit Qoal (see Figure 3.0-1) that consists of older alluvial deposits of gravel and sand and silt atop the Tshirege Member and largely predates incision of canyons on the Pajarito Plateau. The remaining subunits of the Tshirege Member are resistive. The Cerro Toledo interval, Otowi Member, and Puye Formation are conductive, with the Puye Formation being more conductive than the units above it.

One goal of this study was to assess the relative importance of surface water infiltration below mesa tops versus canyon floors. The three north-south profiles (Lines 1, 2, and 3; Appendix A, Figure A-4.1-12) show that a vertical zone of low resistivity penetrates the resistive tuffs in the Tshirege Member beneath CdV at Lines 1 and 2 but not at Line 3. Similarly, Line 5 along the axis of CdV (Appendix A, Figure A-4.1-13) shows that the tuffs beneath the floor of CdV, including normally resistive Tshirege tuffs, have low resistivity west of the intersection with Line 3. These data are consistent with surface water and alluvial well data that indicate the main infiltration pathway for contaminated water in CdV is located downcanyon of the 260 Outfall and extends east to the vicinity of MDA P (Reid et al. 2005, 093660; LANL 2011, 207069).

Small mesa top drainages may also be associated with deep low resistivity anomalies and therefore significant infiltration pathways, as illustrated by the Line 1 results profile (Appendix A, Figure A-4.1-1). Vertical conductive features are associated with the storm drainage for building TA-16-260 at electrode 110 and, to a lesser extent, the 260 Outfall at electrode 76 (Appendix A, Figure A-3.1-1). The anomaly associated with the building TA-16-260 is one of the most prominent electrical features identified in the TA-16 survey and extends to a depth greater than 300 ft. The drainage captures storm water from the parking lot near building TA-16-260, and periodically it contained running water during the survey. Although this drainage is not a source for contaminant infiltration, it illustrates that local areas of increased infiltration can occur on mesas where sufficient hydrologic drivers exist.

Another low resistivity anomaly on a mesa top occurs on the north canyon rim at Line 4 electrode 130 (Appendix A, Figure A-3.1-1). This anomaly is a vertical conductive feature that penetrates the resistive tuffs of the Tshirege Member and become progressively more conductive with depth (Appendix A, Figure A-4.1-7). There is no infrastructure in this area, and the source of this electrical anomaly is not known. The anomaly occurs beneath a tributary stream that drains into CdV and may represent focused infiltration of storm and snow melt runoff (Figures 3.0-1 and A-3.1-1). Alternatively, the anomaly may indicate the presence of a fault that has higher moisture from infiltrating surface water or contains clay associated with fault gouge. However, detailed geologic mapping for this area conducted for the seismic hazards program (Figure 3.0-1; Lewis et al. 2009, 111708) did not identify a fault at this location. It is tempting to correlate the anomaly at Line 4 electrode 130 to similar vertical conductive anomalies in the same vicinity at Line 5 electrode 145 and Line 6 electrode 135 (Appendix A, Figure A-4.1-13), forming a deep-penetrating north-south linear structure. However, the Line 5 anomaly occurs near the deep well at CdV-16-1(i) and is likely affected by the presence of stainless-steel well casing surround by a hydrated bentonite annulus (Kleinfelder 2004, 087844). Similarly, the Line 6 vertical anomaly is located at the cluster of deep wells near well R-25 and is almost certainly the result of highly conductive well casings. R-25, the deepest well in the cluster, is a 1934-ft-deep stainless-steel well, and it contains 70 ft of 13.375-in.-diameter thick-walled drill casing that was abandoned from depths of 508 to 578 ft during the well's construction (Broxton et al. 2002, 072640). The current interpretation is that the anomaly at Line 4 electrode 130 is independent of the anomalies at Line 5 electrode 145 and Line 6 electrode 135 and that the latter two anomalies are the result of manmade infrastructure.

The spatial resolution of the DC electrical resistivity geophysical survey decreases with increasing depth and it is not possible to resolve lower vadose zone features of hydrogeological interest such as perched groundwater zones or significant lithological boundaries (e.g., perching horizons) (Appendix A, section 4.0). At a gross scale, it appears the Puye Formation may be slightly more conductive south of CdV than to the north (Appendix A, Figures A-4.2-8 and A-4.2-9). The Puye Formation is an alluvial fan deposit shed from volcanic highlands to the west and lithologies north and south of CdV should be similar. Higher conductivity values may indicate higher moisture contents and/or more abundant clays, possibly indicating that perched water in the Puye Formation is more likely to occur south of CdV. However, the differences in resistivity values from north to south are very small and may not have much hydrologic significance (Appendix A, Figures A-4.2-8 and A-4.2-9).

The goal to determine if deep-perched groundwater occurs in the Puye Formation north of CdV will be more directly addressed by wells that will be installed in the near future. There are no apparent adjustments for the proposed locations for planned perched intermediate and regional aquifer wells based on the results of this geophysical investigation. Interpretations of these geophysical data will be periodically reevaluated as new subsurface data become available from new deep wells.

4.0   REFERENCES

The following list includes all documents cited in this report. Parenthetical information following each reference provides the author(s), publication date, and ER ID. This information is also included in text citations. ER IDs are assigned by the Environmental Programs Directorate's Records Processing Facility (RPF) and are used to locate the document at the RPF and, where applicable, in the master reference set.

Copies of the master reference set are maintained at the New Mexico Environment Department Hazardous Waste Bureau and the Directorate. The set was developed to ensure that the administrative authority has all material needed to review this document, and it is updated with every document submitted to the administrative authority. Documents previously submitted to the administrative authority are not included.

Broxton, D., R. Warren, P. Longmire, R. Gilkeson, S. Johnson, D. Rogers, W. Stone, B. Newman, M. Everett, D. Vaniman, S. McLin, J. Skalski, and D. Larssen, March 2002. "Characterization Well R-25 Completion Report," Los Alamos National Laboratory report LA-13909-MS, Los Alamos, New Mexico. (Broxton et al. 2002, 072640)

Kleinfelder, May 7, 2004. "Final Well CdV-16-1(i) Completion Report," report prepared for Los Alamos National Laboratory, Project No. 37151/9.12, Albuquerque, New Mexico. (Kleinfelder 2004, 087844)

LANL (Los Alamos National Laboratory), September 2011. "Investigation Report for Water Canyon/ Cañon de Valle," Los Alamos National Laboratory document LA-UR-11-5478, Los Alamos, New Mexico. (LANL 2011, 207069)

LANL (Los Alamos National Laboratory), March 2012. "Technical Area 16 Well Network Evaluation and Recommendations," Los Alamos National Laboratory document LA-UR-12-1082, Los Alamos, New Mexico. (LANL 2012, 213573)

LANL (Los Alamos National Laboratory), April 2012. "Work Plan for Direct Current Resistivity Profiling in Cañon de Valle," Los Alamos National Laboratory document LA-UR-12-20546, Los Alamos, New Mexico. (LANL 2012, 215111)

LANL (Los Alamos National Laboratory), May 15, 2014. "Request for Extension to Submit the Summary Report for Direct Current Resistivity Profiling in Cañon de Valle," Los Alamos National Laboratory letter (EP2014-0183) to J. Kieling (NMED-HWB) from J. Mousseau (LANL) and P. Maggiore (DOE-NA-00-LA), Los Alamos, New Mexico. (LANL 2014, 256573)

Lewis, C.L., J.N. Gardner, E.S. Schultz-Fellenz, A. Lavine, and S.L. Reneau, June 2009. "Fault Interaction and Along-Strike Variation in Throw in the Pajarito Fault System, Rio Grande Rift, New Mexico," *Geosphere,* Vol. 5, No. 3, pp. 252–269. (Lewis et al. 2009, 111708)

NMED (New Mexico Environment Department), May 18, 2012. "Approval, Work Plan for Direct Current Resistivity Profiling in Cañon de Valle," New Mexico Environment Department letter to P. Maggiore (DOE-LASO) and M.J. Graham (LANL) from J.E. Kieling (NMED-HWB), Santa Fe, New Mexico. (NMED 2012, 520404)

NMED (New Mexico Environment Department), May 31, 2013. "Approval with Modification, Drilling Work Plan for Well CdV-9-1(i)," New Mexico Environment Department letter to P. Maggiore (DOE-LASO) and J.D. Mousseau (LANL) from J.E. Kieling (NMED-HWB), Santa Fe, New Mexico. (NMED 2013, 522693)

NMED (New Mexico Environment Department), November 1, 2013. "Second Extension Request to Submit the Summary Report for Direct Current Resistivity Profiling in Cañon de Valle," New Mexico Environment Department letter to P. Maggiore (DOE-LASO) and J.D. Mousseau (LANL) from J.E. Kieling (NMED-HWB), Santa Fe, New Mexico. (NMED 2013, 523814)

Reid, K.D., S.L. Reneau, B.D. Newman, and D.D. Hickmott, August 2005. "Barium and High Explosives in a Semiarid Alluvial System, Cañon de Valle, New Mexico," *Vadose Zone Journal,* Vol. 4, pp. 744–759. (Reid et al. 2005, 093660)
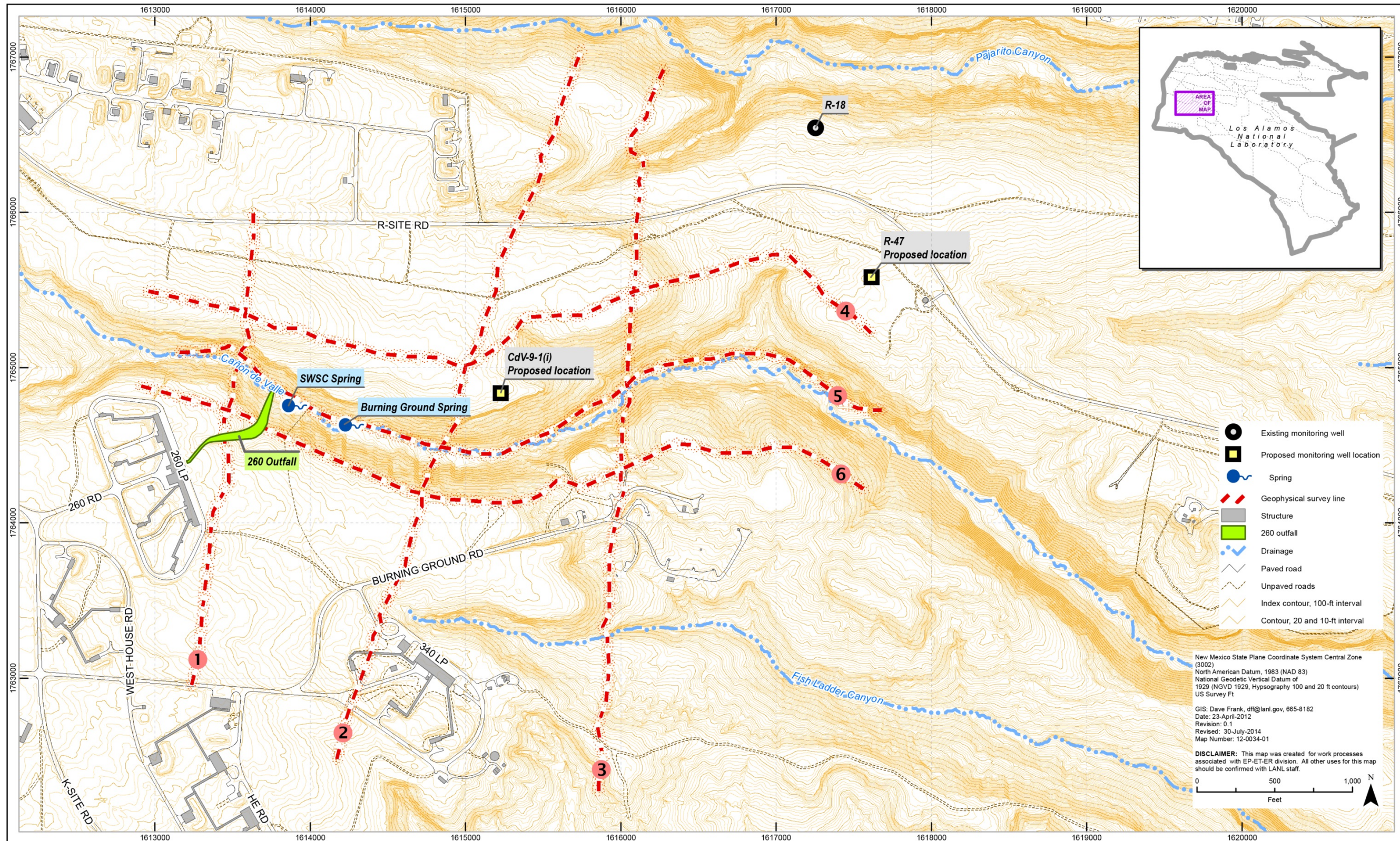
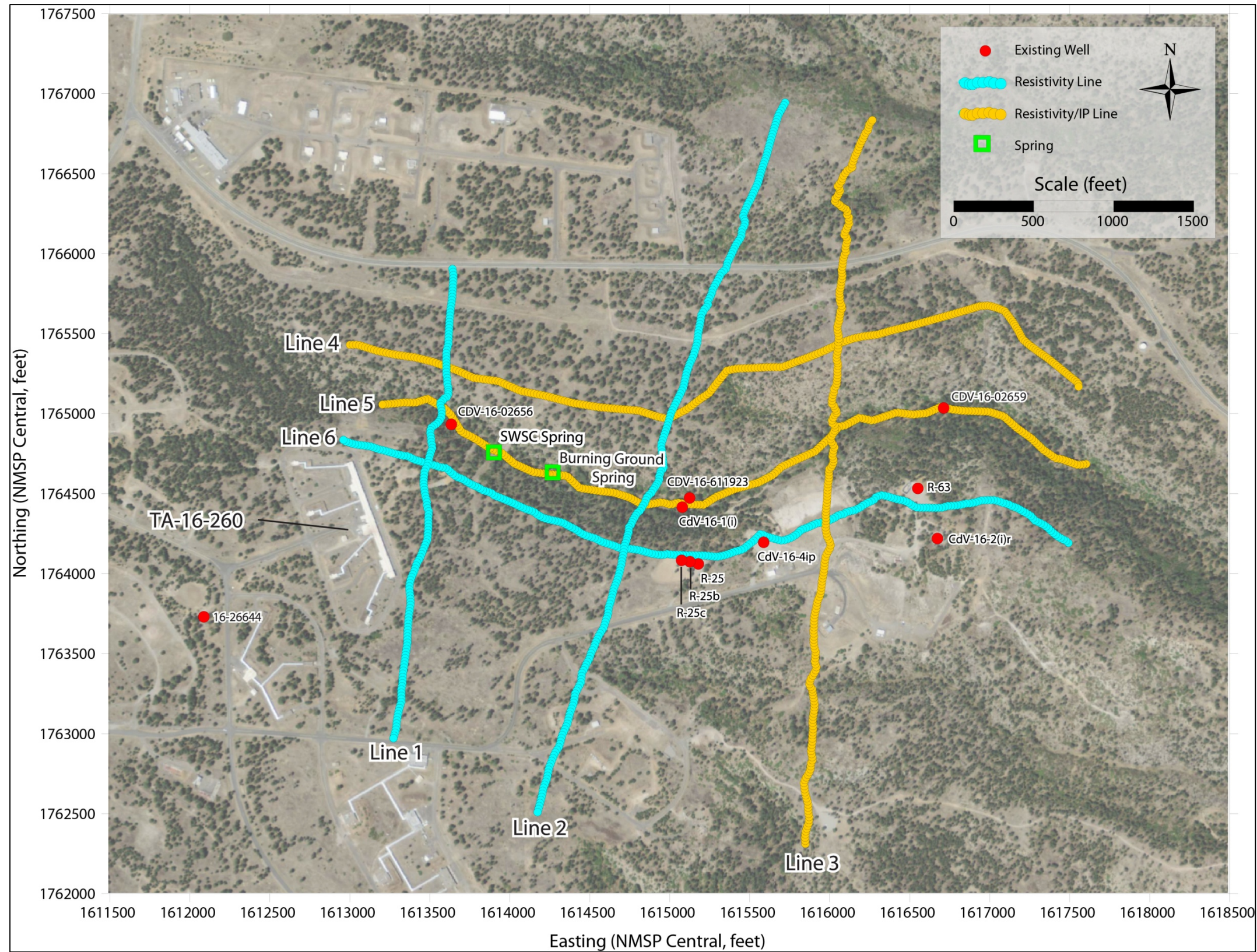**Figure 1.0-1   Location of the study area at the Los Alamos National Laboratory**

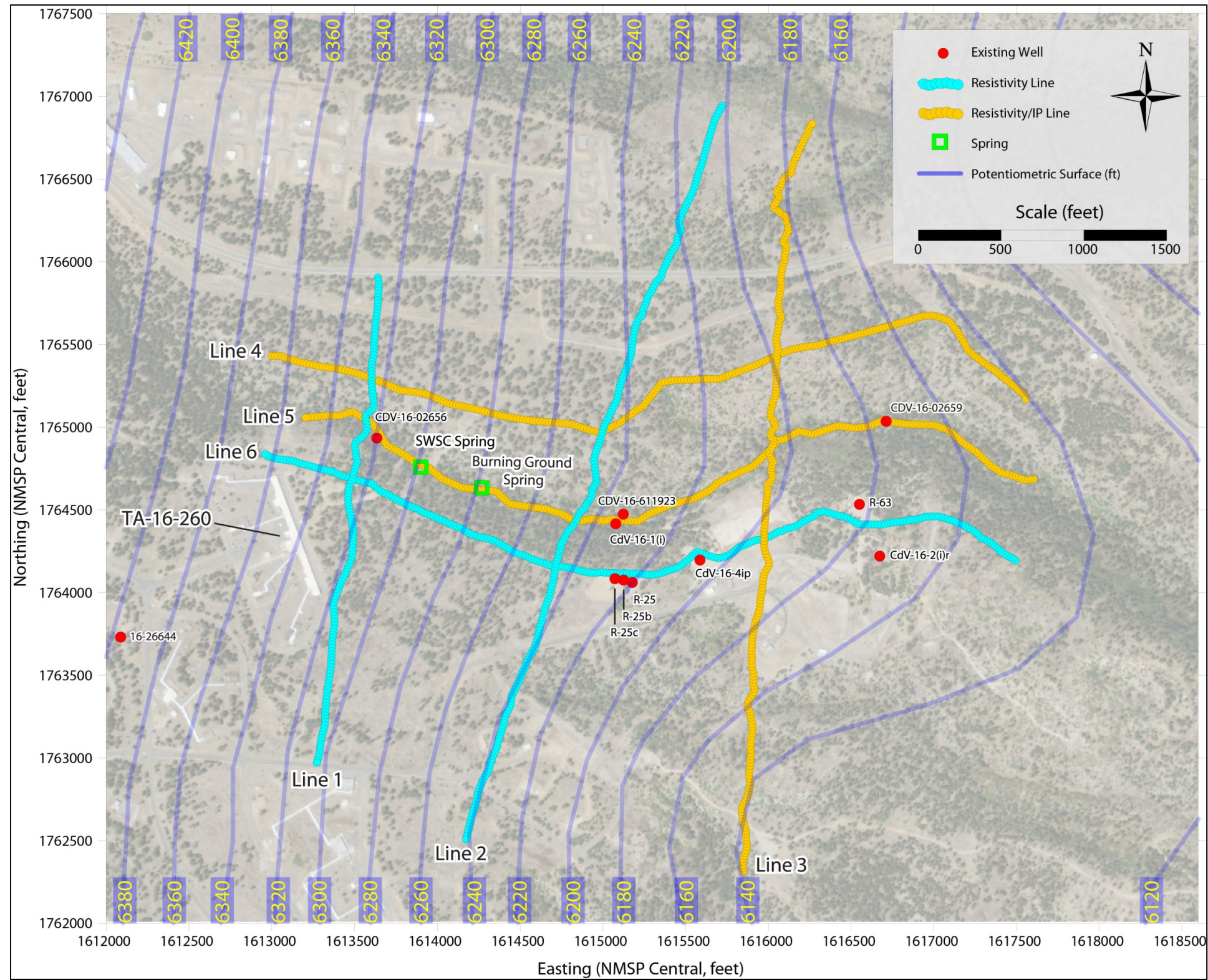**Figure 1.0-2   Resistivity and IP coverage within CdV**

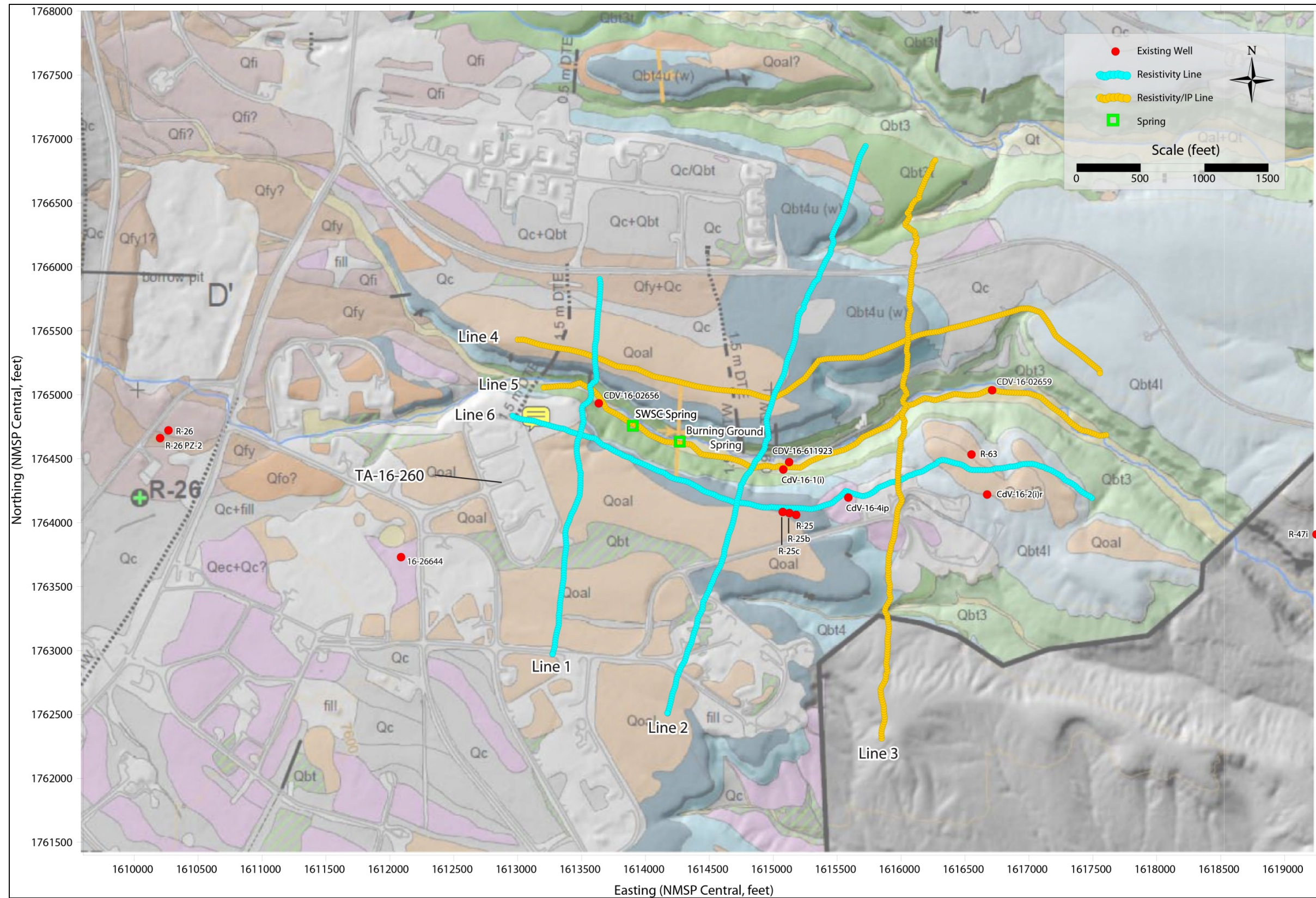**Figure 1.0-3   Potentiometric surface at CdV (modified from LANL 2011, 207069)**

Figure 3.0-1   Surface geology of TA-16

Appendix A

Geophysical Methods and Results

CONTENTS

Tables

A-1.0   INTRODUCTION

The Cañon de Valle (CdV) electrical resistivity investigation (Figure 1.0-1 of the report) included acquiring, modeling (in both two- and three-dimensions), and interpreting six lines of electrical resistivity within and next to CdV at Los Alamos National Laboratory (LANL or the Laboratory) (Figure 1.0-2). Three lines were run parallel to the canyon and were over 5000 ft in length. The remaining three lines were placed perpendicular to the canyon to help tie the features together. In addition, three of the resistivity lines (Lines 3, 4, and 5) had accompanying induced-polarization (IP) measurements to test chargeability effects of the different lithological units. The IP was not part of the original scope but was added during the investigation to enhance understanding of the subsurface. HydroGeophysics, Inc. (HGI) conducted this survey in May and June of 2014.

The main objective of this study was to map the electrical structure of the vadose zone in the vicinity of CdV (LANL 2012, 215111). Of particular interest was the identification of low resistivity regions indicative of increased moisture content, clay-rich zones associated with groundwater pathways, changes in geologic lithologies, or perched water.

A-2.0   BACKGROUND

A-2.1   Previous Geophysical Investigations of CdV

Appendix I of the Investigation Report for Water Canyon/Cañon de Valle (LANL 2011, 207069) includes a summary of several studies conducted in CdV, including a few electrical resistivity lines run by HGI. The surveys were conducted to investigate the infiltration of effluent, groundwater flow, and bedrock properties into and below the Bandelier Tuff. Two resistivity lines were run longitudinal down CdV, and three lines were placed perpendicular to the channel. Figure A-2.1-1 shows the location of the older 2001 survey lines relative to the survey conducted in 2014.

The resistivity data from 2001 was reprocessed with the newer modeling software and placed into context for direct comparison with the 2014 survey. Color scales and lithological units have been preserved for context. Figure A-2.1-2 shows the results of the remodeling effort. It should be noted that the reprocessing of Line 1 only includes the first 1000 ft. The upper portion of the canyon, as represented by Line 1, is more conductive than Line 2. Resistivity targets along the line appear to align well with the lithological boundaries, so one explanation for the transition from conductive to resistive Qbt 2 of the Tshirege Member could be the degree of saturation. At approximately 400 ft along Line 1, there is a narrow zone of lower resistivity that appears to coincide with a mapped fault with 1.5 m of down-to-the-east displacement (Figures 3.0-1 and A-2.1-2). It is not known if this low resistivity zone represents higher moisture from infiltrating surface water or clay associated with fault gouge, or both.

Natural- and controlled-source magnetotellurics soundings (natural source audio-frequency magnetotellurics [NSAMT] and controlled source audio-frequency magnetotellurics [CSAMT], respectively) were undertaken in 2002 and 2003 by Zonge Engineering. The depths of investigation by these methods exceeded 1500 ft. In general, the data confirm that the western portion of CdV is more conductive than the eastern portion, and several low resistivity "pipes" that support evidence of infiltration of water at specific sites and along the western part of Technical Area 16 (TA-16) into the vadose zone.

Borehole wireline geophysical logging was also conducted by Schlumberger within the past 5 yr. The wells included R-63, R-47i, and CdV-16-4ip, with a goal to map borehole properties (deviation, diameter, etc.) and geological and hydrogeological conditions with a number of different tools. Two of the boreholes

are coincident with Line 6 of the present survey, and some of these data are used to directly compare with the electrical resistivity images.

A-2.2   Infrastructure

Figure A-2.2-1 shows a layout of the utilities across the site, including water, sewer, electric, and gas lines. Utilities have the potential to interfere with electrical resistivity and IP data depending on the construction material, depth, diameter, and electrical grounding. For example, polyvinyl chloride (PVC) pipelines would not cause interference with the imaging but steel or cast iron will. Buried electrical lines with insulation also should not cause interference. It is not known what the exact construction material is for each of the pipelines. Sewer and water lines are typically PVC. Older gas lines may be made of steel, whereas newer lines may be a type of plastic. Buried electrical lines will be electrically insulated, but overhead power lines may be grounded at each pole, thus providing a potential electrical source.

Deep wells with stainless-steel casing surrounded by an annulus of hydrated bentonite are located in CdV and on the mesa south of CdV. These wells are electrically conductive and have the potential to interfere with electrical resistivity and IP data.

A-3.0   METHODOLOGY

A-3.1   Survey Area and Logistics

Data along two-dimensional (2-D) profiles within CdV were obtained between May 13, 2014, and June 5, 2014. The acquisition of electrical resistivity data involves injecting current into the ground between two electrodes and measuring the electrical potential between two other electrodes, repeated for multiple combinations of the available electrodes. The specific combination is referred to as an array, and for final data analysis and interpretation the Wenner array was used. The Schlumberger array (SLB) was tested on a few lines and was found to be too noisy for the depth of investigation (>1200 ft). The Schlumberger array employs a fixed and closely spaced transmitting dipole, and the Wenner array employs an expanding transmitting dipole. The expanding transmitting dipole used in the Wenner array keeps the geometric factor low and hence has a larger signal-to-noise ratio for a comparative resistivity value.

A total of six 2-D profiles were collected. A detailed survey layout is shown in Figure A-3.1-1, which includes electrode numbers for later reference. Table A-3.1-1 lists the geographic details of the profiles.

A-3.2   Equipment

Data were collected using a Supersting R8 multichannel electrical resistivity system (Advanced Geosciences, Inc., Texas) and associated cables, electrodes, and battery power supply. The Supersting R8 meter is commonly used in surface geophysical projects and has proven itself to be reliable for long-term, continuous acquisition. The stainless-steel electrodes were laid out along profiles with an electrode spacing that varied between 16.5 ft (5 m) and 20 ft (6 m). The mixing of electrode spacings was a consequence of different cable inventories needed to create deep profiles. Multielectrode systems allow for automatic switching through preprogrammed combinations of four electrode measurements.

Electrode locations were surveyed using a Garmin hand-held global positioning system. Elevations for each electrode were then obtained from digital elevation model (DEM) data provided for the area and incorporated into the subsequent inverse modeling.

A-3.3   Data Processing

Measurements of electrical resistivity with electrical resistivity tomography systems inevitably contain errors from a variety of sources, including poor electrode contact, random device errors, and external effects. An assessment of these errors provides some means of quality control of the data. The process of data editing identifies and eliminates erroneous data points, but no data modification (rounding, averaging, smoothing, or splining) is performed.

The recorded electrical resistivity data were downloaded each day for analysis. Error statistics are computed within the Supersting R8 for multiple readings (or stacks) on each electrode configuration. The error values on these multiple readings are used as rejection criteria, where data with errors greater than 5% were removed from the data set. Additional important diagnostic data parameters from the raw data include voltage/current (V/I, or transfer resistance, in ohms), voltage (volts), and electrical current (amps) output. The rationale is to find and remove spurious points that do not conform to the data population or points that violate potential theory. The aim was to remove data outside of the statistical population–measurements with negative V/I, low voltage (<0.01 V), or low current (<10 mA) were removed from the data set.

The data were inverse modeled using the Res2Dinv and Res3Dinv software packages. The software uses an "Occam's" style inversion, which produces a smooth model of the subsurface electrical resistivity that fits the acquired data within certain tolerances. The inversion proceeded in an iterative manner until the data misfit was below an acceptable level, 10% for all cases presented in this report. An inherent assumption of 2-D inverse modeling is that the resistivity in the cross-line direction is constant. At sites with complex resistivity structure, the 2-D assumption may introduce significant error, and the resulting 2-D images can contain significant distortions. Hence, in areas with the potential for complex three-dimensional (3-D) electrical targets (i.e., faults, fractures, perched water tables) whose dimensions out of the plane of the 2-D resistivity profile cannot be assumed to remain constant, it is possible that distortions will be observed in the resulting inversion models. The distortions can take the form of under- or overestimation of the modeled resistivity value of features, location errors for electrical conductive features, or incorporating out-of-plane features into the 2-D profiles.

One method to reduce the distortions caused by the 2-D assumption is to incorporate the individual 2-D profile data into a 3-D inverse model. This was achieved using the Res3Dinv software package. The data from the individual 2-D profiles were georeferenced and incorporated into a 3-D grid format. The outline of the 3-D grid is shown in Figure A-3.1-1. The 3-D inverse modeling included a total of 30,976 measurements. Several trials were run that changed model grid cell size from 100 ft × 100 ft to 200 ft × 200 ft. Other trials included adding layers to the model corresponding to the different lithological units and the water table. The resulting output resistivity model was subsequently processed and visualized using the Surfer (Golden Software, Inc., Golden, Colorado) and Rockworks (Rock Ware, Inc., Golden, Colorado) software.

A-4.0   RESULTS

A-4.1   2-D Resistivity Profile Results

The 2-D resistivity model results are presented as 2-D profiles in Figures A-4.1-1 to A-4.1-2, A-4.1-4 to A-4.1-10, A-4.1-12 to A-4.1-13. Common color-contouring scales were used throughout, and there is no vertical exaggeration in the 2-D profile figures. Electrically conductive (low-resistivity) subsurface regions are represented by cool hues (purple to green), and electrically resistive regions are represented by warm hues (orange to red). To help emphasize particular features in each section, a log scale of model resistivity is used in the profile figures. When data span multiple orders of magnitude, it is appropriate to display a log transformation. Table A-4.1-1 lists the data statistics for each profile.

Annotated 2-D profiles are also presented in Figures A-4.1-1 through A-4.1-10. The locations of the points of intersection for the various profiles are indicated along the ground surface contour for reference. In addition, fault and monocline locations are indicated by colored diamonds along the ground surface contour; these were taken from the regional geological map of Lewis et al. (2009, 111708) (Figure 3.0-1). They are used for comparison with interpreted features in the model resistivity profiles. Lastly, the stratigraphic boundaries (from Weston-Cole 2011 model) are drawn along the profiles at their relevant locations and depths.

Fracture, fault, and fissure mapping with electrical resistivity is fairly common and has been discussed in numerous studies. The main component to finding these structural features is the offset in model resistivity contouring or a large change in resistivity values along a lineation consistent with a change in geology. Considering the small throws along the faults identified in the geological map (Figure 3.0-1), it is assumed a fault is present based on an offset in model resistivity contours. However, it cannot be determine if low resistivity associated with faults and fractures is the result of increased water content compared with surrounding material, or it represents higher clay content associated with fault gouge.

Borehole investigations within the survey area have identified perched water at several locations. In CdV, shallow perched groundwater typically occurs within welded bedrock tuffs along nearly horizontal partings and depositional boundaries. Within the electrical resistivity profiles, perched groundwater is expected to be represented by horizontal lenses of low resistivity, based on the increase in the degree of saturation in these normally unsaturated geological units.

In general, the six profiles display a number of comparable features across the surveyed area. First, there is a general lateral trend, where the very near surface representing alluvial material and perhaps weathered and nonwelded Qbt 4 of the Tshirege Member of the Bandelier Tuff is conductive. There are also conductive isolated targets in the near surface that can be related specifically to hydrological features (building drainage, springs, and standing water in the canyon). The remaining portion of the Tshirege Member is resistive. Deeper units, including the Cerro Toledo interval, Otowi Member of the Bandelier Tuff, and Puye Formation, are conductive. The three lines oriented generally south to north have infrastructure effects from buried or overhead power lines.

2-D Resistivity Line 1

Figure A-4.1-1 shows the results of Line 1, which was the shortest line run perpendicular to CdV. As a consequence, the depth of investigation was approximately 700 ft and into the Cerro Toledo interval. The line shows a conductive near-surface layer, likely resulting from Quaternary alluvium with retained moisture and weathered material of Qbt 4 of the Tshirege Member. The next layer is resistive and appears to correlate with Qbt 3 and Qbt 4 of the Tshirege Member. The geological map shows these layers nearly horizontal across the line, but the resistivity data suggest the beds tilting downward towards the axis of CdV. Units Qbt 3 and Qbt 3t of the Tshirege Member are moderately to densely welded ash-flow tuffs in this part of the Laboratory. Qbt 4 of the Tshirege Member is nonwelded to densely welded ash-flow tuffs. The lower part of Qbt 4 is nonwelded to partly welded and contains intercalated surge deposits. The upper part of Qbt 4 includes densely welded ash-flow tuffs that form mesa caprock. The degree of welding and low moisture may contribute to the resistive nature of the material.

Within this resistive layer are conductive breaks that correspond to hydrological sources, such as building drainage at electrode 110, the 260 Outfall at electrode 76, and the location of the stream channel within CdV. The building drainage source releases storm water and perhaps runoff from the parking lot near TA-16-260 and active drainage was periodically occurring during the survey.

The lower subunits of the Tshirege Member, including Qbt 1 and Qbt 2, show a slightly more conductive layer. The increase in conductivity extends into the Cerro Toledo interval at the base of the profile.

2-D Resistivity Line 2

Figure A-4-1.2 shows the results of Line 2, which is located east of Line 1 and runs perpendicular to CdV. Line 2 was significantly longer than Line 1 and therefore imaged deeply into the Puye Formation. The near surface shows a thin layer of conductive material that is coincident with the information of Line 1 and could be the result of porous alluvial material with a moderate amount of moisture combined with the weathering of the top surface of Qbt 4 of the Tshirege Member. The next layer down is resistive. Here, the high resistivity extends through all of the Tshirege Member. The lower boundary of the Qbt 1g of the Tshirege Member correlates with the transition back to lower resistivity material near the intersection of Line 4. Below the Tshirege Member, the Cerro Toledo interval, Otowi Member, and the Puye Formation all become progressively more conductive.

At a few intervals along the line, there are extreme conductivity signatures starting from the surface that are coincident with infrastructure and utilities. The infrastructure includes overhead power lines at electrodes 83, 184, and 224 as well as a concrete vault at electrode 233. Two of the power lines (electrodes 83 and 183) appear to severely impact the resistivity structure associated with the geological strata, making the interpretation of the section uncertain with respect to the conductivity signature in the lower formations. One potential method to remove these effects is to eliminate portions of data collected at the infrastructure location.

Electrode removal was attempted on Line 2 by removing data associated with electrodes 79 to 87 and 181 to 188. The data count was reduced from 6176 to 3557, and Figure A-4.1-3 shows the data distribution along the line for the full and reduced data set. The data are presented as a pseudosection of points associated with each individual four-pole measurement.

Figure A-4.1-4 shows the resulting inversion for the reduced dataset. The low resistivity target on the south side of CdV shifted slightly northward and the removal seemed to have no effect on the overall structure. For the target on the north side, the near surface (upper 200 ft, to the base of Qbt 3 of the Tshirege Member) returns to a higher resistivity much like the material nearby. The deeper portion of the conductive target, however, is retained suggesting that perhaps an even greater amount of data should be eliminated, although the elimination of too much data will affect other aspects of the model.

2-D Resistivity Line 3

Figure A-4.1-5 shows the resistivity model for Line 3. The section shows a three-layered system, where the uppermost layer is conductive and likely represents moisture retained in alluvial material and weathered Qbt 4 of the Tshirege Member. The middle resistive layer represents the remaining subunits of the Tshirege Member. It is likely the interface between the Tshirege Member and Cerro Toledo interval could be shifted deeper directly beneath the canyon, based on the high resistivity material contours. The material below the Tshirege Member, including the Cerro Toledo interval, Otowi Member, and Puye Formation, appear to be more conductive.

Infrastructure in the area affects the results at both ends of the line. Overhead power lines and buried pipelines create extremely conductive signatures between electrodes 88–98 and at electrode 190.

A time-domain IP test was conducted along Line 3 (Figure A-4.1-6). The Wenner array was again used for the acquisition but this time using a broader separation of electrodes (skipping every other electrode compared with the full Wenner acquisition presented above). IP can be collected alongside resistivity by

measuring the decay of the voltage when the electrical current is switched off. The IP measures charge storage, and materials that can store charge will have a slower decay. The measured apparent chargeability values are presented as an integrated voltage value over the time window divided by the primary voltage just before the current is switch off; hence, the units are in time (in this case milliseconds). The data are then inverted with the apparent resistivity to produce a section of chargeability.

Although the IP method is most often used in mapping sulfidic deposits (ore-comprising pyrite, chalcopyrite, chalcocite, covellite, or bornite), volcanic materials can exhibit strong IP signatures as well. Figure A-4.1-6 shows the results of the IP acquisition across CdV with a repeat of the resistivity on top and chargeability below. The resistivity signature is very similar to that of Figure A-4.1-5. The chargeability data show lateral variability across the section, with higher values just south of the canyon and directly below Line 4 location. The cause of the high chargeability is not known.

2-D Resistivity Line 4

Figure A-4.1-7 shows the results of the chargeability and resistivity for Line 4. The line was acquired with a larger electrode spacing (double the normal spacing from 20 to 40 ft). Line 4 is the first line without significant infrastructure, so the layering of resistivity corresponding to the different strata can be viewed without interference. The resistivity shows the three-layered structure is generally retained, with a thin conductive surface layer that is especially prominent west of the intersection with Line 2. This thin conductive surface layer appears to correlate with alluvial deposits and less welded portions of Qbt 4 of the Tshirege Member. Deeper portions of the Tshirege Member are resistive, with the basal Qbt 1 of the Tshirege Member marking the transition to more conductive material. At the center of the line is a prominent vertical low resistivity anomaly. This anomaly extends down to the Puye Formation and become more conductive with depth.

The chargeability data generally shows a transition from low to high with depth. The transition is marked by the base of Qbt 3 of the Tshirege Member. This type of IP signature may indicate an inductive interference between adjacent wires within the cables carrying the time-dependent voltage or between the cables and conductive ground. There is a lateral transition from west to east, with the east becoming more chargeable. The highest chargeability is directly east of the low resistivity signature.

2-D Resistivity Line 5

Figure A-4.1-8 shows the resistivity results of Line 5, which was acquired along the axis of CdV; hence, Qbt 4 of the Tshirege Member is missing. The line is more conductive than other lines. The normally resistive Tshirege Member transitions from low to high resistivity near the intersection of lines 5 and 3 (Figure A-4.1-8). As the cross lines indicate, Lines 1 and 2 (Figures A-4.1-1 and A-4.1-2) show bedrock beneath the canyon floor to be conductive, coincident with Line 5. Line 3 also agrees with Line 5 at their intersection. According to pole-pole data collected in 2001 (Figures A-2.1-1 and A-2.1-2) the two sections also show the material transitioning from a conductive west to a resistive east (LANL 2011, 207069). Lastly, the material below the Tshirege Member is conductive across the entire line. A more conductive Cerro Toledo interval, Otowi Member, and Puye Formation is consistent across all lines.

The most prominent feature of the line is vertical conductive feature that occurs approximately 2100 ft along the line at electrode 145. The feature extends below a fault as mapped in Figure 3.0-1. There is a marked similarity to the vertical conductive feature observed along Line 4. Other near surface hydrological features also exhibit resistivity lows, such as the two springs at the upper end of the canyon and standing water in the stream bed.

Figure A-4.1-9 shows the results of an IP test conducted on Line 5. Again, these data were collected at a much broader electrode spacing than resistivity alone. IP takes a significantly longer time to acquire, so these tests were down-sampled during acquisition to keep the field acquisition schedule. The resistivity data shown in Figure A-4.1-9 match that of Figure A-4.1-8. The chargeability data show a slight increase in values from the surface down to the Puye Formation, with a break at approximately 2600 ft along the line. The slightly higher chargeability on the western side is coincident with the low resistivity vertical signature and could indicate either potential interference from the well CdV-16-1(i) which is steel-cased and reaches a depth of 658 ft. Alternatively, the low resistivity vertical structure may represent clayey material filling a fault. The IP results of Line 3 and Line 5 at their intersection appear to agree.

2-D Resistivity Line 6

Figure A-4.1-10 shows the last 2-D profile acquired at CdV, which was acquired on the south mesa of CdV. Line 6 shows an opposite trend in resistivity signature compared to Line 5, with a resistive west end and a conductive east end. A vertical low resistivity anomaly occurs near electrode 135 at the cluster of wells near well R-25. Well R-25 is a 1934-ft-deep stainless-steel well and contains 70 ft of 13.375-in.-diameter thick-walled drill casing that was abandoned from depths of 508 to 578 ft during the well's construction (Broxton et al. 2002, 072640). The well cluster at R-25 is likely a source of infrastructure interference, producing the vertical anomaly in the resistivity signal. This anomaly appears to be on strike with similar vertical conductive features in Lines 4 and 5, but these anomalies may be unrelated, as discussed in section 3.0 of this report. The eastern portion of Line 6 may be conductive simply because of the amount of buried infrastructure in the area. The road at 2900 ft distance along the line, for example, shows a very conductive signature. Figure A-2.2-1 does not show any buried pipelines at this location.

Wireline borehole geophysical logs were conducted at R-63 (LANL 2011, 204541) and CdV-16-4ip (LANL 2011, 111608). At these locations, the inverted resistivity sections cover depths of 376 and 824 ft, respectively. The wireline data extended to below 1200 ft, and much of the nearer-surface data were not collected or were not usable for direct comparison with the resistivity. A comparison that can be made, however, is with the moisture data within CdV-16-4ip, and Figure A-4.1-11 compares side-by-side the resistivity at that location and the water content/saturation data. The figure shows the moisture starting to significantly increase at a depth of approximately 600 ft, with the moisture as high as 20% at a depth of 670 ft. The resistivity shows a slight drop near that interval.

2-D Resistivity Composites

Figure A-4.1-12 and A-4.1-13 show composites of parallel lines to help explain consistent electrical features across the site. Figure A-4.1-12 aligns Lines 1 through 3 with the canyon. All three lines show a bowl-shaped resistive Tshirege Member directly beneath the canyon floor. The base of Qbt 1g of the Tshirege Member reflects this shape. The deepest portion of Lines 2 and 3 penetrate the upper portion of the Puye Formation. One of the objectives of the survey was to map the upper perched water system in this formation. Both lines show it to be the most conductive unit and more conductive south of the canyon relative to the north.

For the parallel lines that run from west to east (Lines 4 through 6 in Figure A-4.1-13), the Tshirege Member is mostly resistive. However, the upper western portion of CdV, directly in the canyon floor, appears to be more conductive (as shown in Line 5). The higher conductivity could be a direct influence of the surface water from various springs, runoff, and discharge that could influence the conductivity in this area. A strong vertical feature extends across all lines at approximately the same strike with that of Line 4 (Figure A-4.1-7).

A-4.2   3-D Resistivity Results

After filtering and processing each of the 2-D profiles across the site, all electrode positions in all six lines were georeferenced within the New Mexico State Plane coordinate system. The direct advantage of modeling these data in 3-D is that the offline electrical resistivity features (especially conductive features) will be appropriately accommodated in space, the nonlinear line layout will be modeled in a proper 3-D environment, and targets that extend across multiple lines can be viewed more accurately. The drawback to a 3-D model is the lower resolution and lower detail associated with a grid network that is much larger than the 2-D models. For example, the grid cells for the profiles were on the order of 20 ft, whereas the 3-D model had cell sizes on the order of 200 ft.

Figure A-4.2-1 shows the resistance data versus geometric factor for the six lines. There are 25,034 data values comprising the plot. The geometric factor is calculated as follows:

$$K = 2\pi \left(\left| \frac{1}{\overline{AM}} \right| - \left| \frac{1}{\overline{AN}} \right| - \left| \frac{1}{\overline{BM}} \right| + \left| \frac{1}{\overline{BN}} \right| \right)^{-1}$$

where electrical current transmission electrodes are located at positions A and B and voltage measurement electrodes are at M and N. The geometric factor incorporates a distance measure for the four poles used in making each resistance measurement. Basic potential field theory would dictate that the resistance should drop for an increasing geometric factor and Figure A-4.2-1 shows this behavior. The data distribution also confirms a clean data set. Lastly, the data align within a relatively wide band between apparent resistivity values of 80 ohm-m and 1100 ohm-m. Apparent resistivity (ρ_a) is calculated by

$$\rho_a = K \cdot R$$

where R is the measured resistance as voltage/current.

The boundary of the 3-D model is shown in Figure A-3.1-1. The boundary covers a 4800- × 4800-ft area. The area was then discretized into cells with easting and northing dimensions of 200 ft; there were 25 cells in each direction. For layering of the 3-D model, the upper layers were thinner than the deeper layers to accommodate a reduced sensitivity with depth. The thinnest layers were 10 ft for the first layer, increasing to 20, 50, and 100 ft. The model extended to 1200 ft below ground surface. The topography was also incorporated into the model using the 10-ft DEM data.

The data were incorporated into the software RES3DINVx64, a 64-bit platform for modeling large and complex resistivity data sets. The software features special data and model dampening criteria to ensure spurious data noise does not cause large model uncertainties. It also allows for other a priori information, such as the location of specific electrical boundaries known through other sources. The inclusion of boundaries decouples the electrical layers and provides for sharper contrasts at the layer boundary.

The first trial model was a simple test case to ensure the model would converge to a solution. It included topography, but no stratigraphic boundary information. The final root mean square (RMS) error was 5.9% after the fourth iteration. The RMS error describes the goodness of fit between modeled resistance and measured resistance, and a lower value is ideal. The RMS should represent the expected level of noise for the data set, and hence the error value is expected to be below 5%.

Figure A-4.2-2 through A-4.2-4 show horizontal slices through the domain that represent the surficial material (Figure A-4.2-2), Qbt 2 (elevation 7250 ft, Figure A-4.2-3), and near the top of the Puye Formation (elevation 6550 ft, Figure A-4.2-4). The surficial data show a distribution of intermediate values

(from 160 ohm-m to 630 ohm-m), with the lowest resistivity material likely representing higher moisture in the near surface alluvium and weathered Qbt 4 of the Tshirege Member. The slice through Qbt 2 in Figure A-4.2-3 shows a more extreme distribution of resistivity values. Through the canyon, the eastern part is more resistive compared with the western part. The most conductive material on the south side of the canyon likely represents infrastructural interference. The bottommost plot of the upper Puye Formation shows an elongated north-south trending conductive feature on the south side of the canyon. This feature may be partly influenced by infrastructure, but as the 2-D profiles demonstrate, there could also be an influence by perched groundwater.

Figure A-4.2-5 shows a series of profiles through the 3-D model, located approximately at the northing location that corresponds to Lines 4 through 6. The horizontal slices show the locations of each profile. The contacts of major stratigraphic layers are also shown. The profiles show that the Tshirege Member almost aligns with the high resistivity layer. Below the Bandelier Tuff, the sections become more conductive. The northern most profile shows a conductive feature beneath Line 3. This feature is slightly shifted eastward relative to the 2-D profile of Line 4 (Figure A-4.1-7) and is an example of how bodies are more appropriately positioned in 3-D models.

A second trial for 3-D modeling was conducted by explicitly including the lower boundary of the Tshirege Member as a priori data to allow a decoupling of resistivity properties across this interface. This is a logical break in the model given how strongly the resistivity signature is for the stratigraphic layer. The data set was also filtered to remove data related to infrastructure. The data removal followed the same procedures presented for the 2-D profile modeling, where data associated with particular electrodes were deleted. Figures A-4.2-6 through A-4.2-9 present the horizontal and vertical slices through the model at the same locations as that of Trial 1. Trial 2 model becomes insensitive below an elevation of about 6300 ft. The surficial layer in both trials is nearly identical (Figure A-4.2-6). In the layer representing Qbt 2 (Figure A-4.2-7) the Bandelier Tuff, the high- and low-resistivity values are more dampened relative to Trial 1 (Figure A-4.2-2) when data associated with infrastructure were removed. However, the general shape of the different electrical bodies is preserved. In the Puye Formation, the low-resistivity feature appears more directed to the south side of the canyon (Figure A-4.2-8).

The profiles through Trial 2 of the 3-D model (Figure A-4.2-9) show how the lower boundary of the Tshirege Member is preserved more naturally. The infrastructure effects also appear more limited to the Tshirege Member, thus helping to bring more certainty to the electrical properties of the Cerro Toledo interval and Puye Formation.

A-5.0   DATA SUMMARY

An electrical resistivity survey was conducted in the upper portion of Cañon de Valle to map electrical structure of the vadose zone at depths where deep-perched groundwater is known to occur. The electrical resistivity was supplemented with IP along three of the six lines. The depth of investigation for the survey was in excess of 1000 ft and reached the top of the Puye Formation. The following set of conclusions can be drawn from the survey.

- The deep-resistivity data were clean, likely based on the use of the Wenner array in acquisition. The Schlumberger array was first tested before the Wenner array, but the data from the Schlumberger array were too noisy. The difference between the two arrays can basically be summarized by the Schlumberger array having a fixed and closely spaced transmitting dipole and the Wenner having an expanding transmitting dipole. The expanding transmitting dipole keeps the geometric factor low and hence larger signal-to-noise for a comparative resistivity value.

- The acquired IP data were also clean but needed significantly more filtering based on the lowered sensitivity of the equipment compared with higher-powered resistivity/IP acquisition systems.

- The vadose zone exhibits a layered electrical structure. The near-surface alluvium and weathered subunit Qbt 4 of the Tshirege Member of the Bandelier Tuff are conductive. The remaining subunits of the Tshirege Member are resistive. The Cerro Toledo interval, Otowi Member, and Puye Formation are conductive, with the latter more conductive than the units above it.

- There appear to be infrastructure effects within the data caused by traversing areas with buried pipelines, overhead power lines, and wells. The infrastructure may be masking the true electrical signature related to geologically and hydrologeologically based subsurface structure. Steps were taken to eliminate the infrastructure's influence, specifically by removing data from electrodes near it. These steps had limited success.

- In a related issue, surficial water sources (building drainage, springs, etc.) may affect deep-resistivity values. An example is seen along Line 1, where drainage from TA-16-260 appears quite deep in the profile.

- The profile that appears to have the least amount of infrastructural effects is Line 4. The line showed a vertical conductive feature midway through the line, penetrating the Tshirege Member. The anomaly occurs beneath a tributary stream that drains into CdV and may represent focused infiltration or the presence of a fault.

- Resistivity data acquired in 2001 by HGI along the canyon floor match those acquired along Line 5 for the present survey. Namely, the Tshirege Member appears resistive to the east and conductive towards the upper end in the west. Given the time lag between data sets and the different arrays used, the continuity of the data raises confidence in the data acquired.

- The IP data showed a progression of low values in the near surface to high values at depth. Lateral variability was also observed in the deeper high values. Although the progression may indicate some electromagnetic coupling between adjacent wires within the cable or between the wires and ground surface, the lateral variability at depth helps to identify a relative change across the section (even if the true values are not representative). Line 4, for example, shows a stronger IP response in the east compared with the west and may indicate more competent tuff.

- A 3-D model using data generated from the individual profiles was successfully completed. The success was judged by the convergence of the model to a low RMS error within a few iterations, the degree of continuity in difference resistive and conductive targets, and the geological realism in the results. The 3-D model displayed the same type of layering as demonstrated in the 2-D profiles but allowed individual targets to be more appropriately positioned given the curvature of the surface lines and the effects from offline features.

A-6.0   REFERENCES

The following list includes all documents cited in this appendix. Parenthetical information following each reference provides the author(s), publication date, and ER ID. This information is also included in text citations. ER IDs are assigned by the Environmental Programs Directorate's Records Processing Facility (RPF) and are used to locate the document at the RPF and, where applicable, in the master reference set.

Copies of the master reference set are maintained at the New Mexico Environment Department Hazardous Waste Bureau and the Directorate. The set was developed to ensure that the administrative authority has all material needed to review this document, and it is updated with every document submitted to the administrative authority. Documents previously submitted to the administrative authority are not included.

Broxton, D., R. Warren, P. Longmire, R. Gilkeson, S. Johnson, D. Rogers, W. Stone, B. Newman, M. Everett, D. Vaniman, S. McLin, J. Skalski, and D. Larssen, March 2002. "Characterization Well R-25 Completion Report," Los Alamos National Laboratory report LA-13909-MS, Los Alamos, New Mexico. (Broxton et al. 2002, 072640)

LANL (Los Alamos National Laboratory), January 2011. "Completion Report for Intermediate Well CdV-16-4ip," Los Alamos National Laboratory document LA-UR-11-0187, Los Alamos, New Mexico. (LANL 2011, 111608)

LANL (Los Alamos National Laboratory), July 2011. "Completion Report for Regional Well R-63," Los Alamos National Laboratory document LA-UR-11-3673, Los Alamos, New Mexico. (LANL 2011, 204541)

LANL (Los Alamos National Laboratory), September 2011. "Investigation Report for Water Canyon/Cañon de Valle," Los Alamos National Laboratory document LA-UR-11-5478, Los Alamos, New Mexico. (LANL 2011, 207069)

LANL (Los Alamos National Laboratory), April 2012. "Work Plan for Direct Current Resistivity Profiling in Cañon de Valle," Los Alamos National Laboratory document LA-UR-12-20546, Los Alamos, New Mexico. (LANL 2012, 215111)

Lewis, C.L., J.N. Gardner, E.S. Schultz-Fellenz, A. Lavine, and S.L. Reneau, June 2009. "Fault Interaction and Along-Strike Variation in Throw in the Pajarito Fault System, Rio Grande Rift, New Mexico," *Geosphere,* Vol. 5, No. 3, pp. 252–269. (Lewis et al. 2009, 111708)
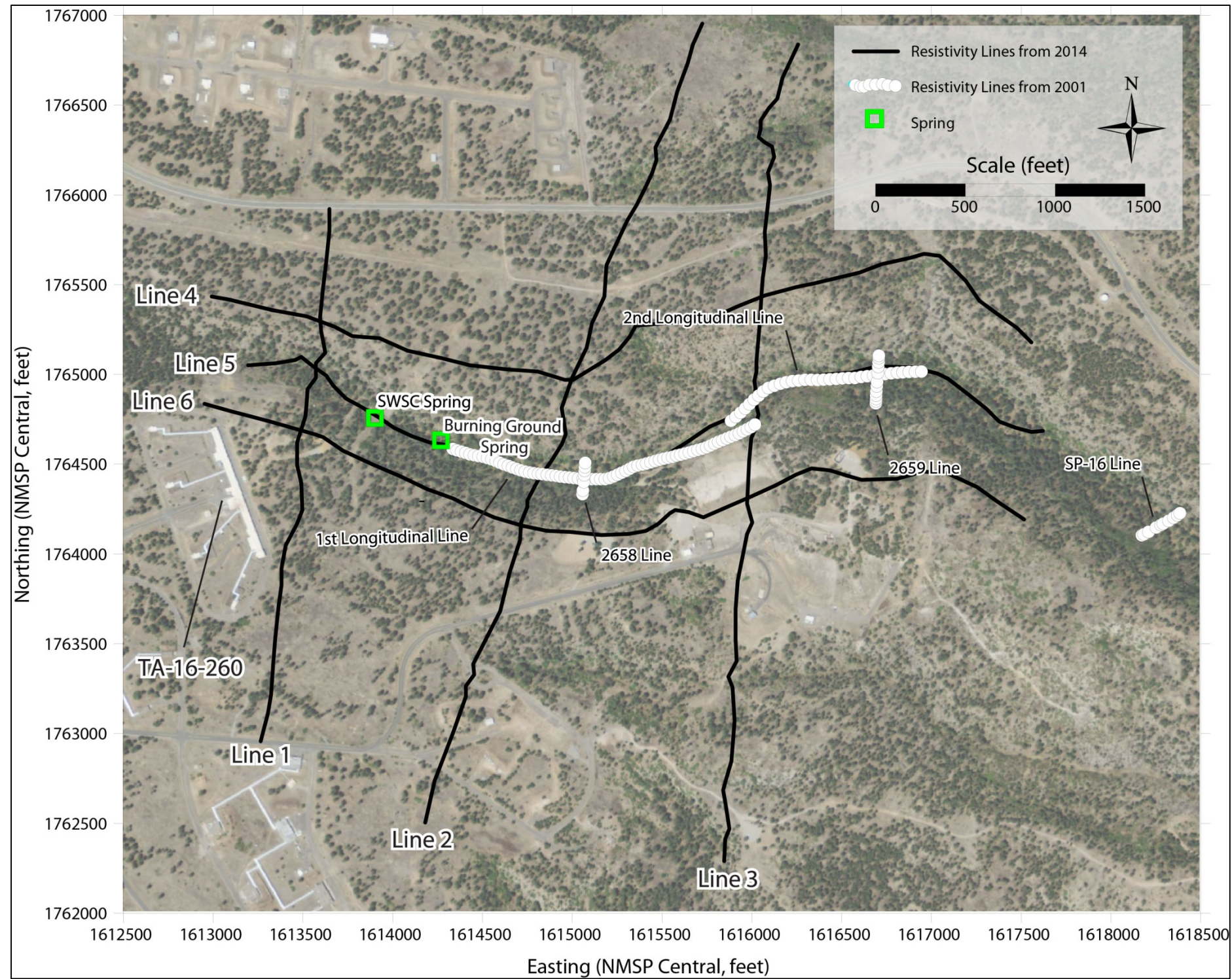
Figure A-2.1-1   Geophysical survey locations in 2001 and 2014
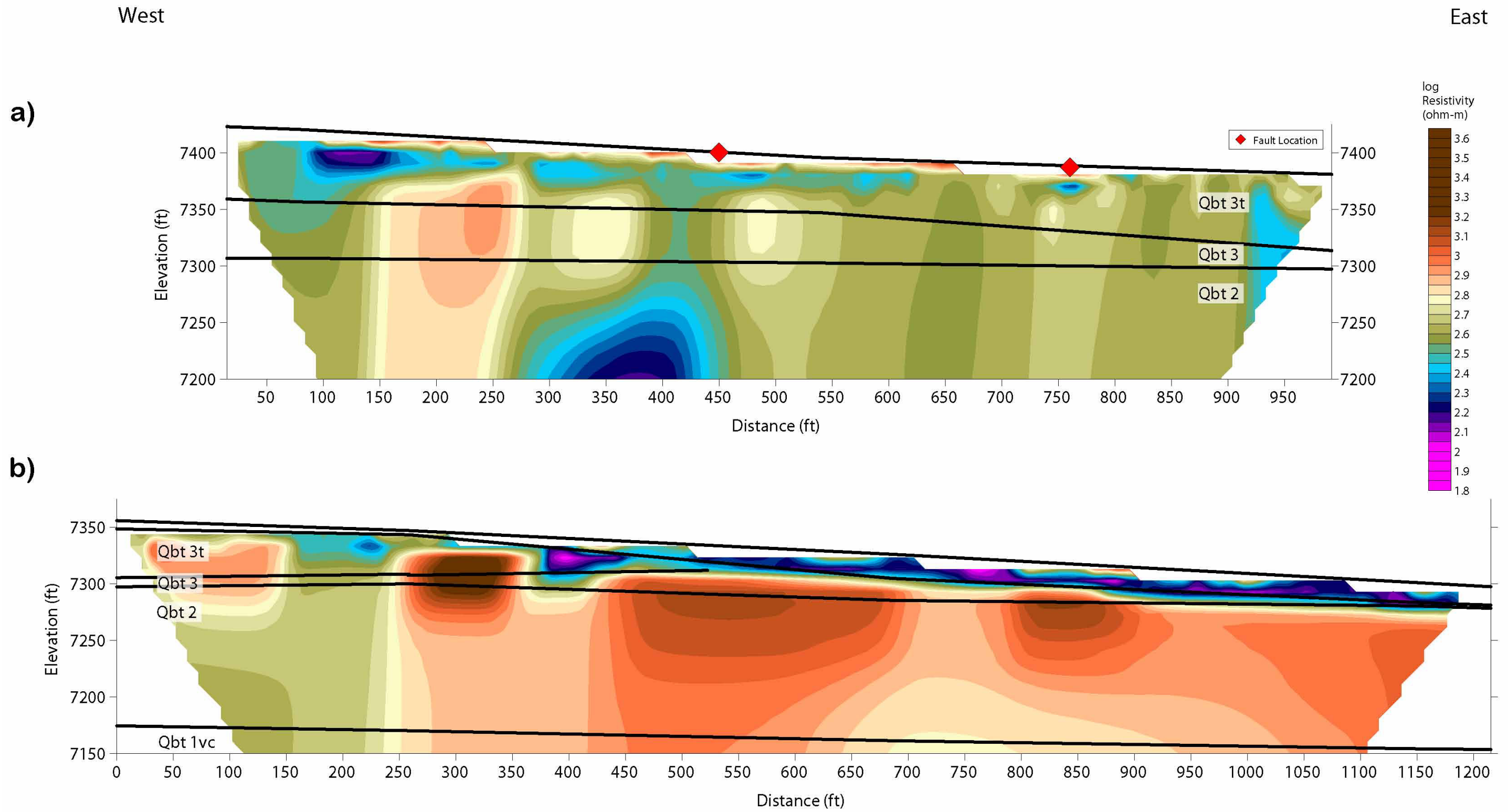
Figure A-2.1-2   Electrical resistivity results of the 1st and 2nd longitudinal lines from 2001
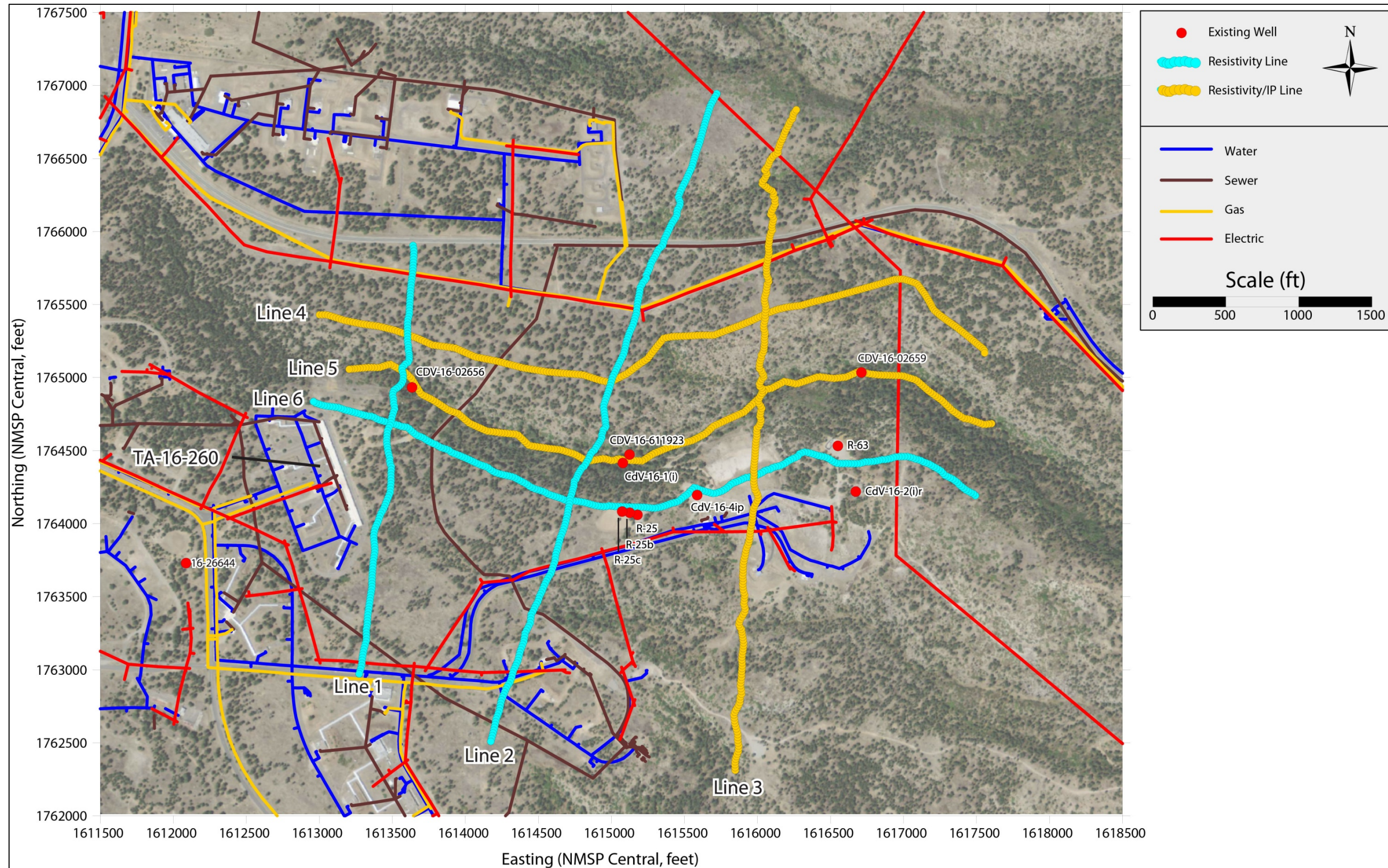
Figure A-2.2-1   Utilities across the survey area
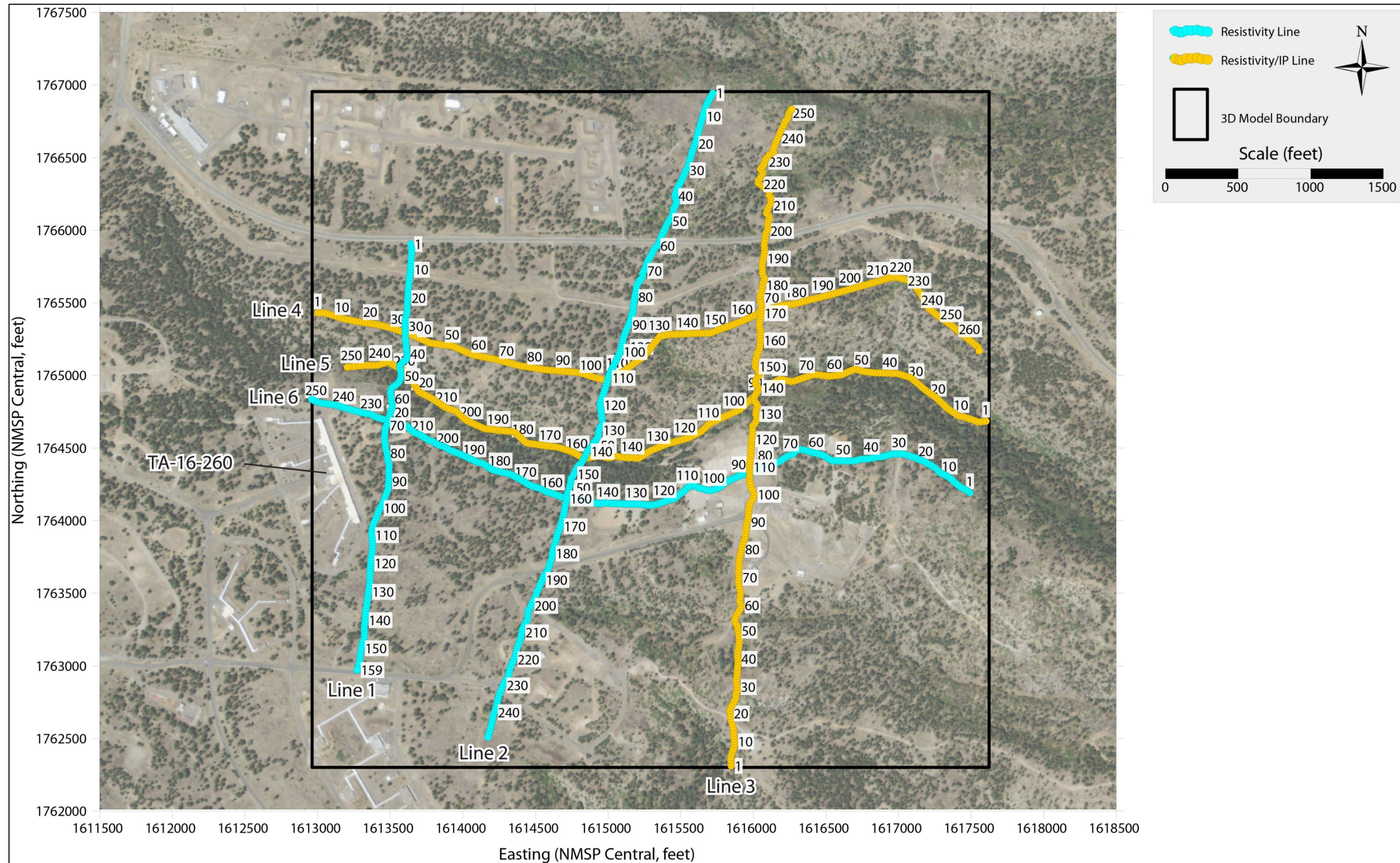
Figure A-3.1-1   Detailed layout of electrode positions for the geophysical survey in CdV
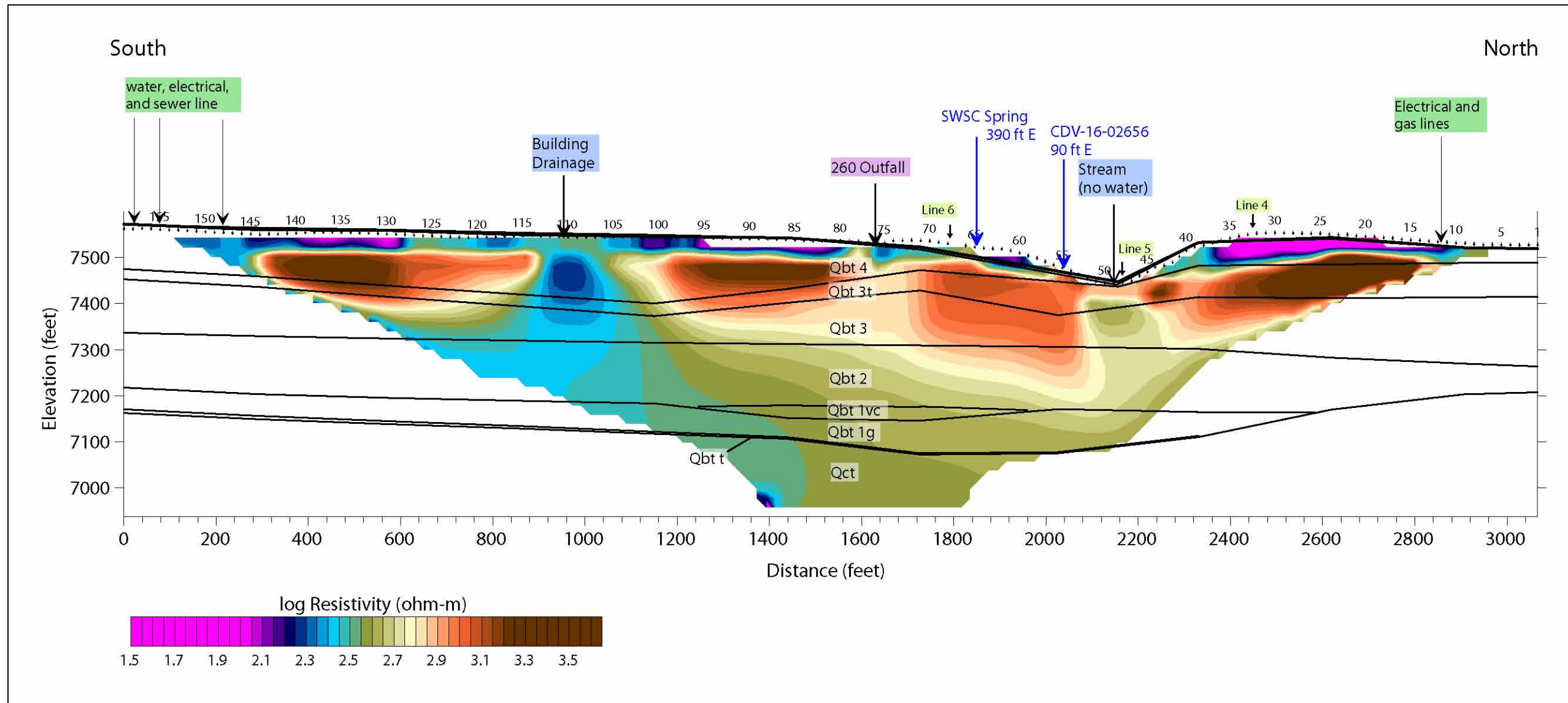
Figure A-4.1-1   Line 1 model resistivity results
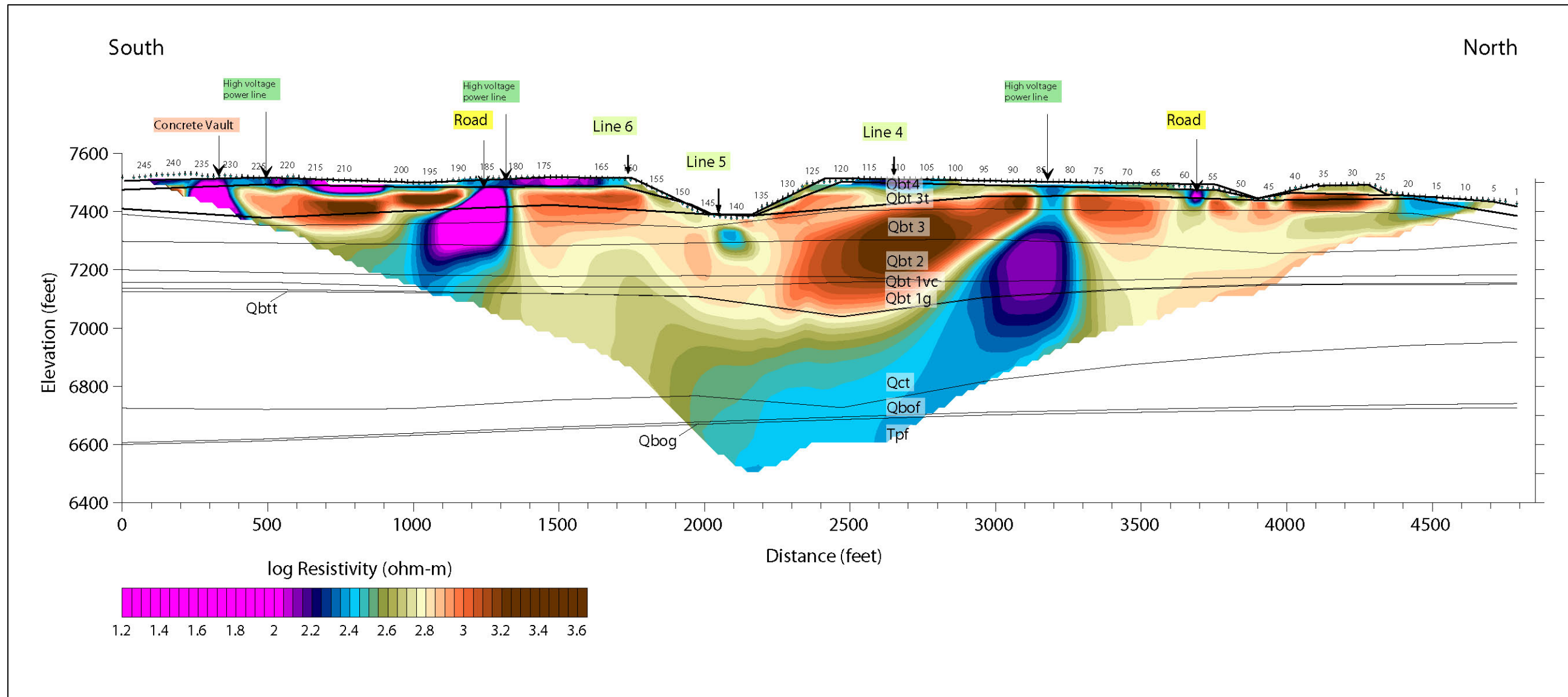
Figure A-4.1-2   Line 2 model resistivity results
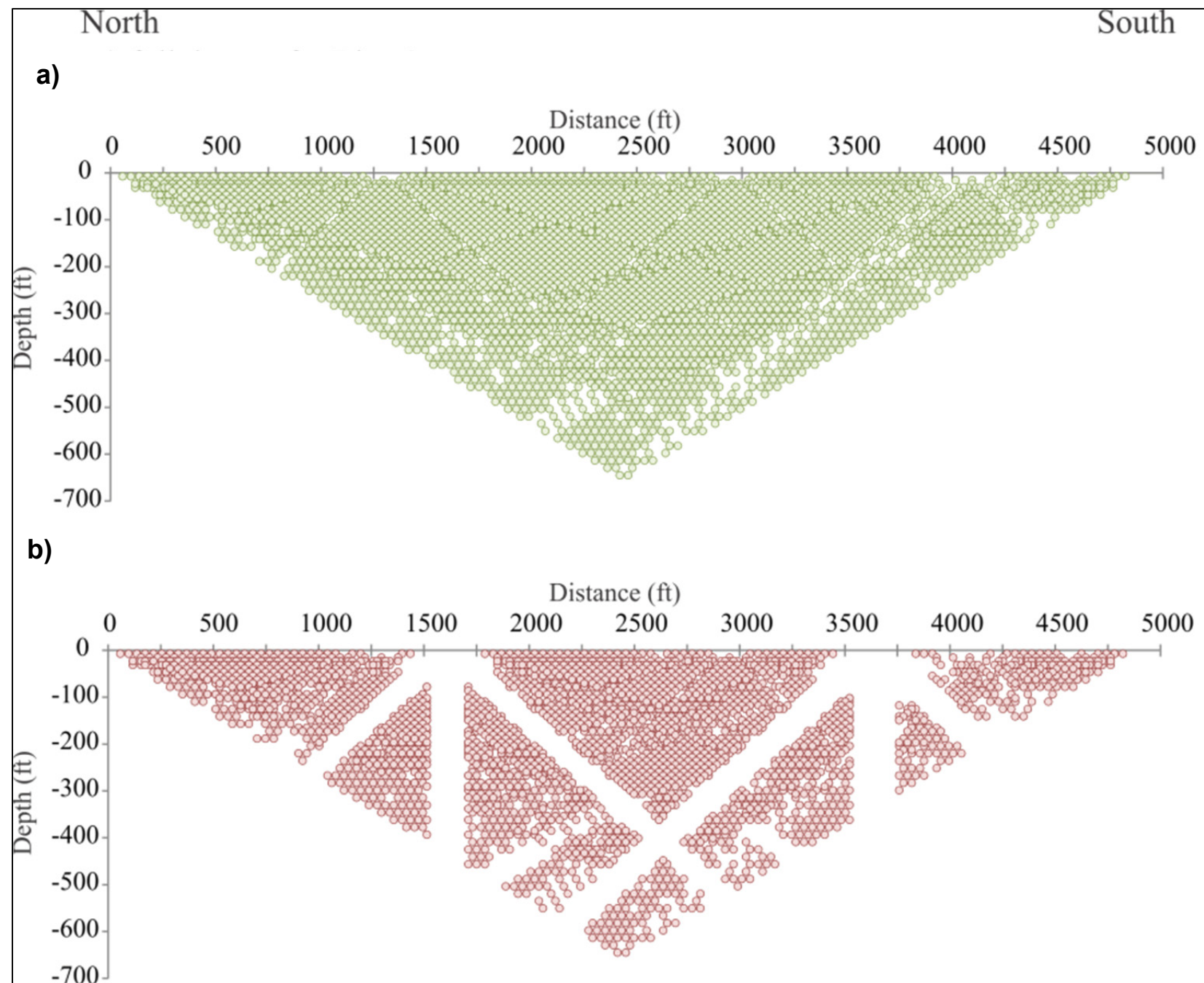
Figure A-4.1-3   Data reduction associated with infrastructure for Line 2: (a) Full dataset for Line 2, and (b) reduced data set for Line 2, eliminating electrodes associated with infrastructure. Note the data are presented as north to south, as collected in field.
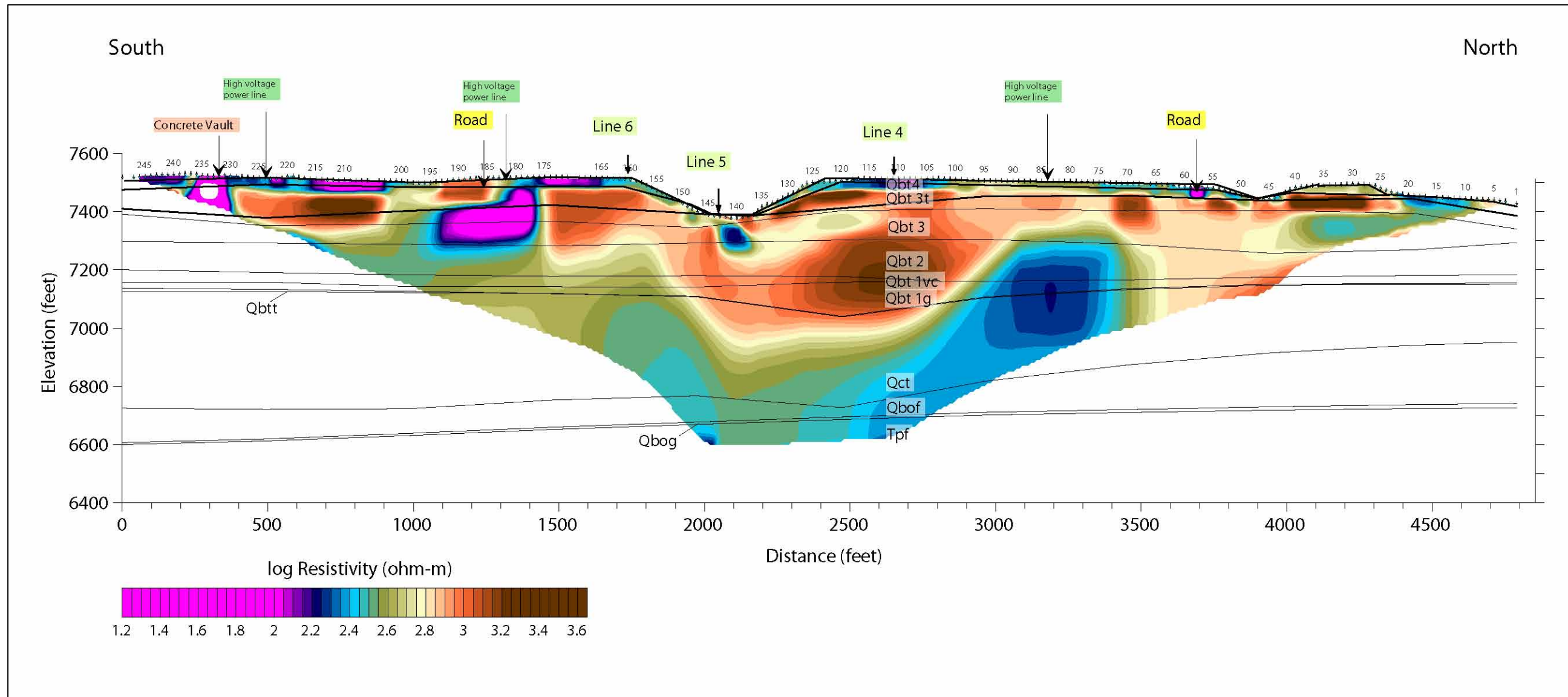
Figure A-4.1-4   Line 2 model resistivity results with reduced data
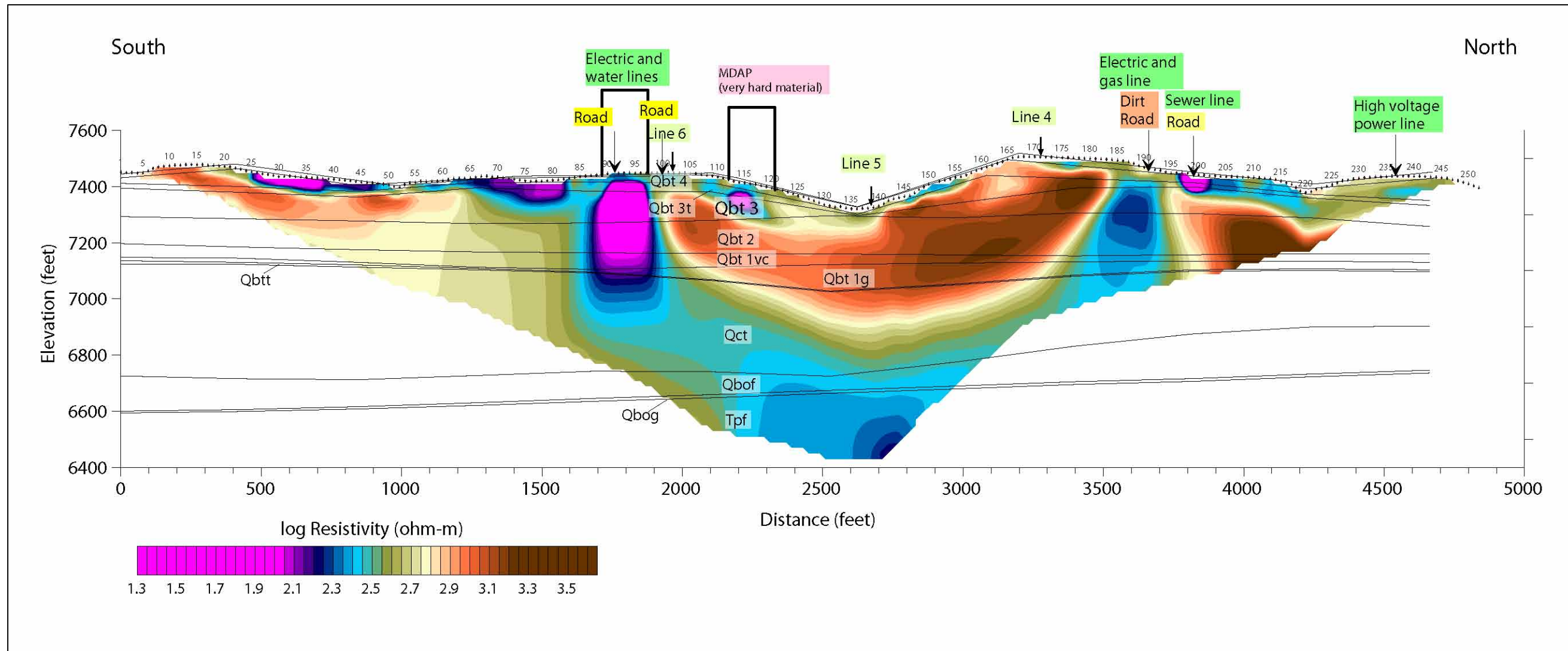
Figure A-4.1-5   Line 3 model resistivity results
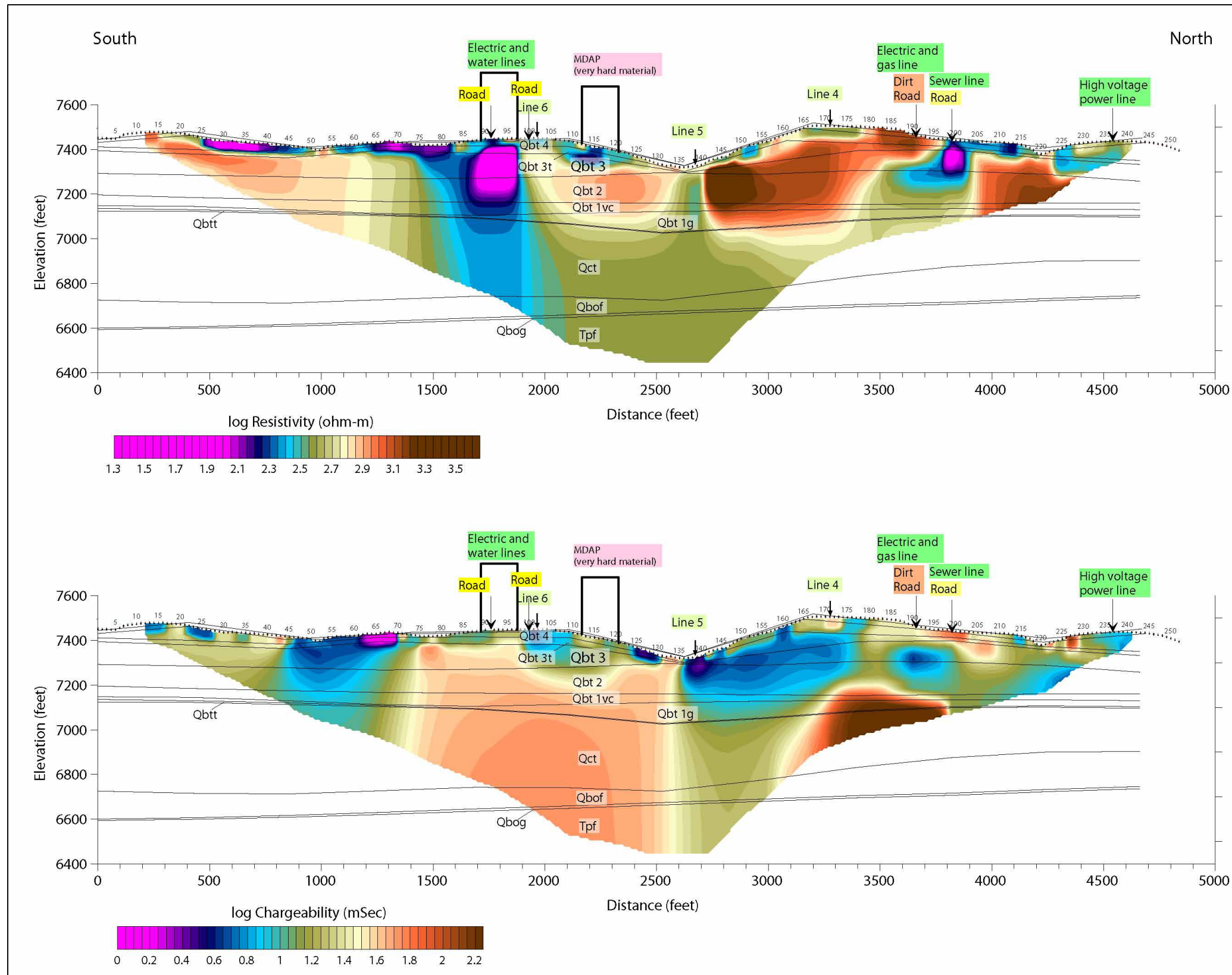
Figure A-4.1-6   Line 3 model IP results
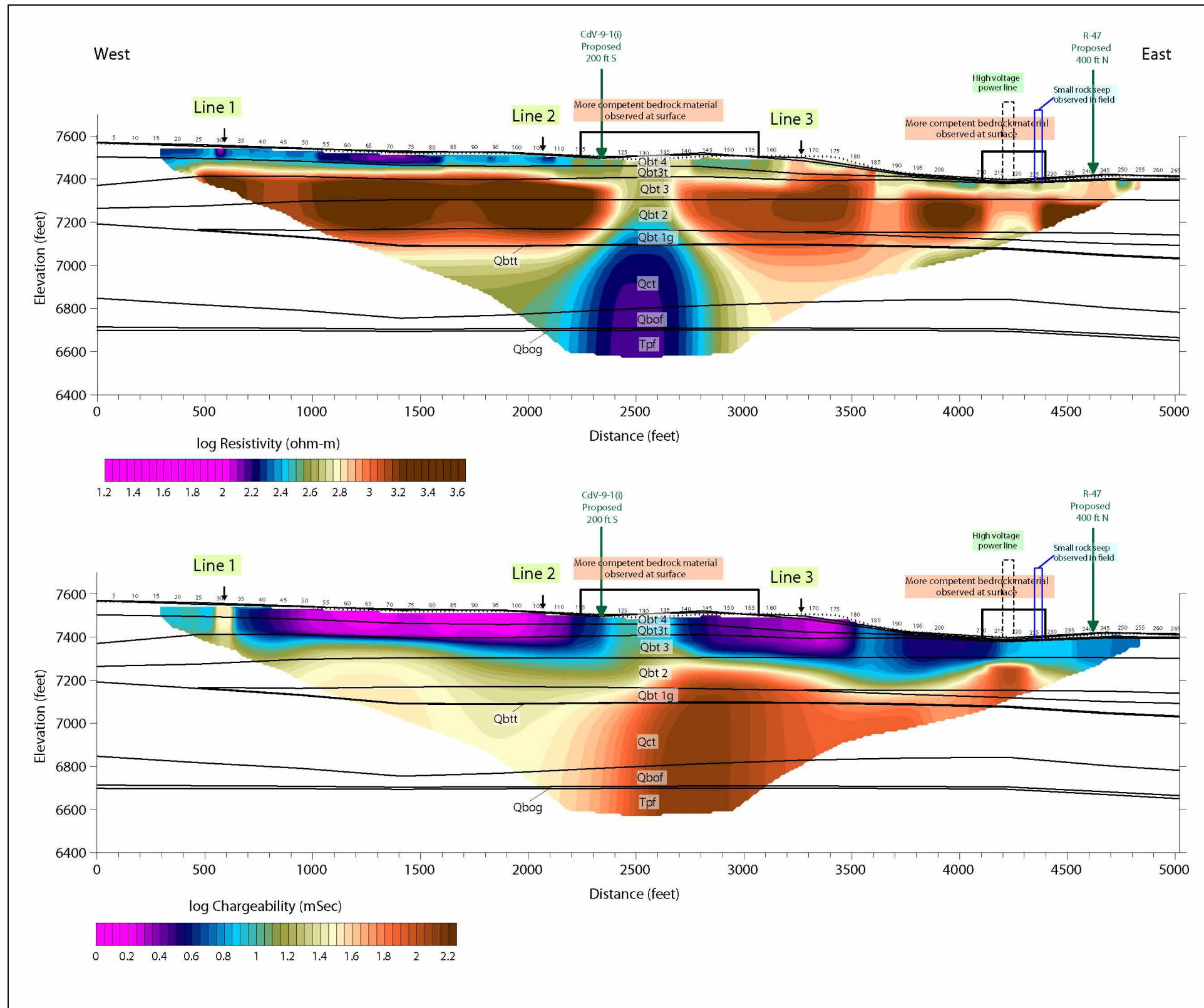
Figure A-4.1-7   Line 4 model resistivity and IP results
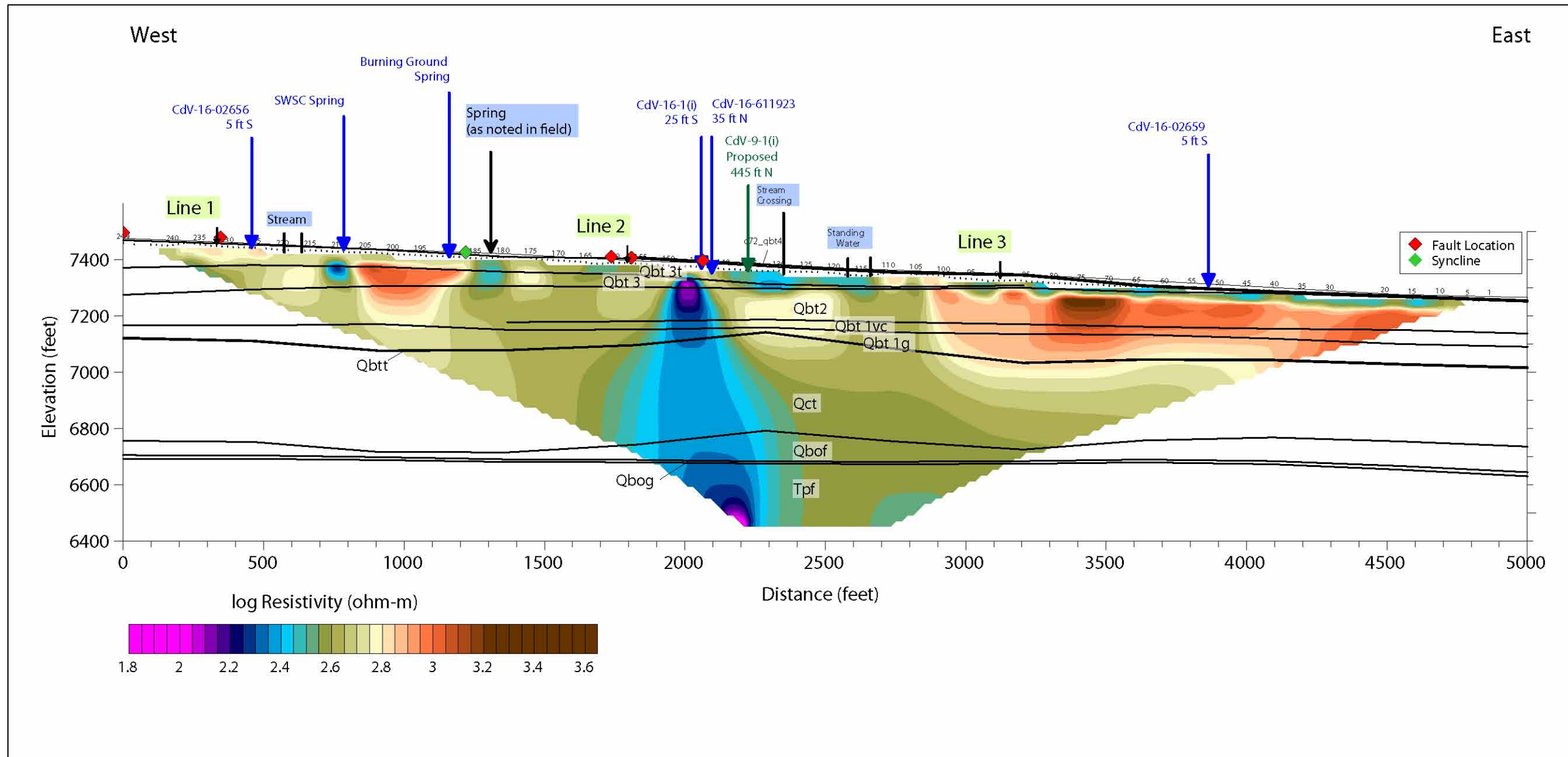
Figure A-4.1-8   Line 5 model resistivity results
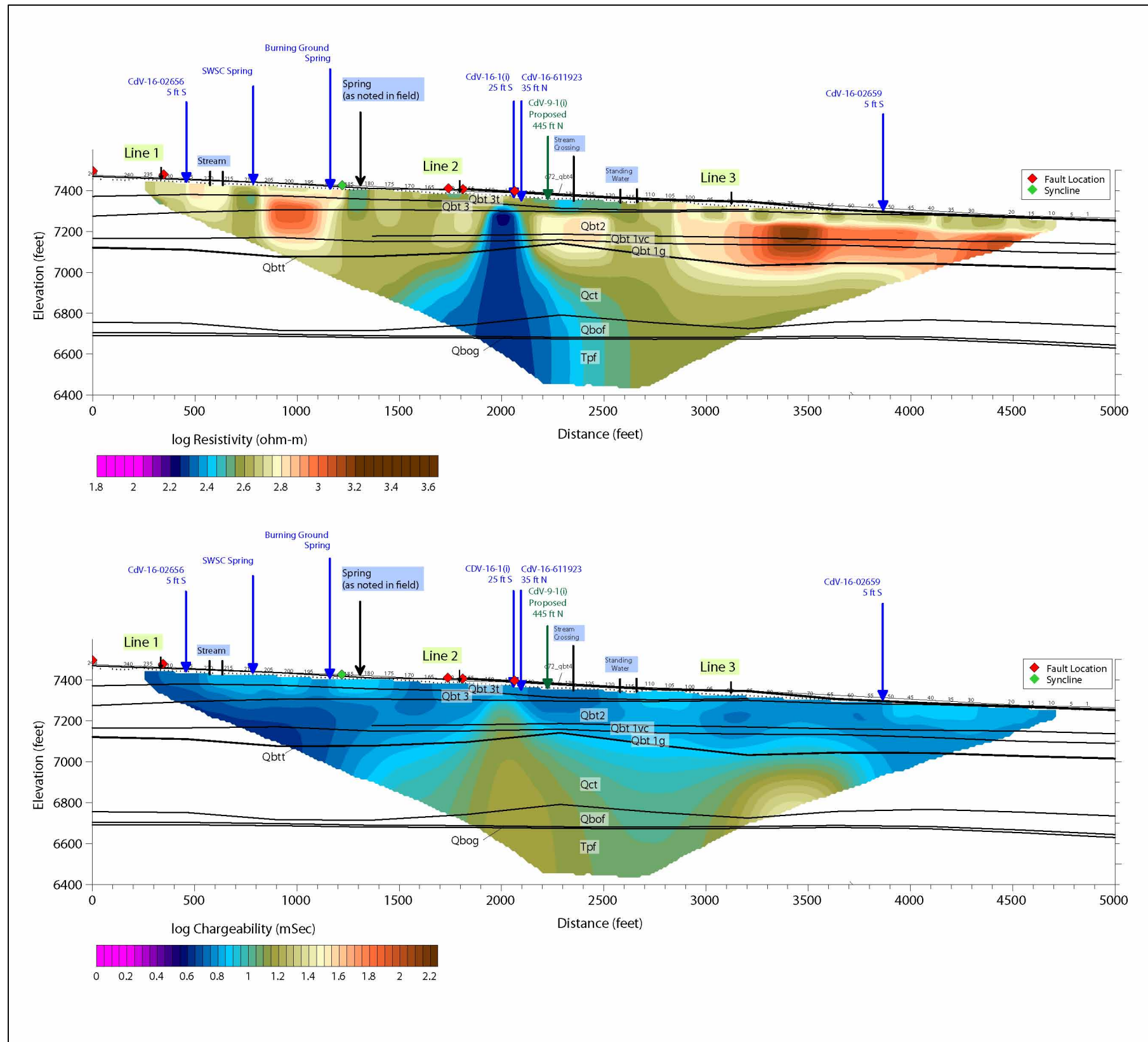
Figure A-4.1-9   Line 5 model resistivity and IP results
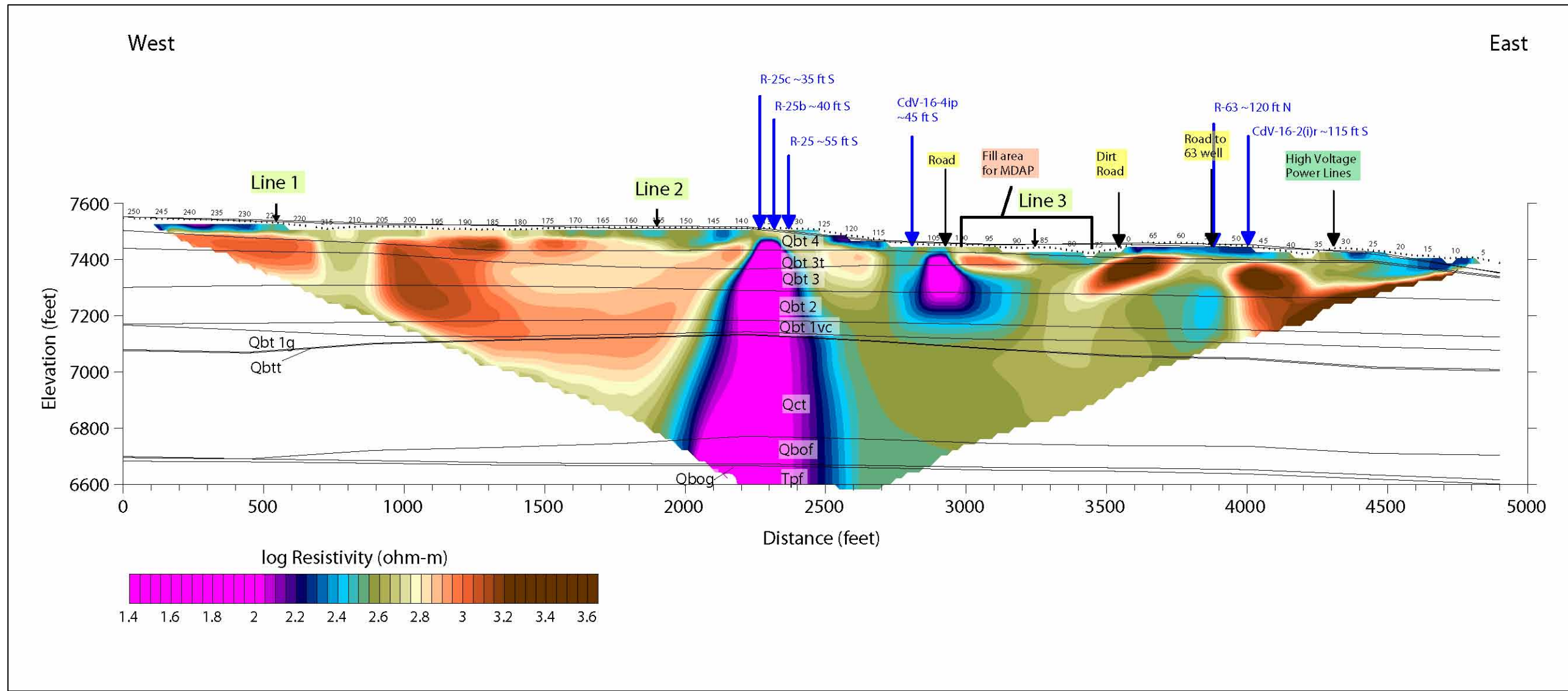
Figure A-4.1-10   Line 6 model resistivity results
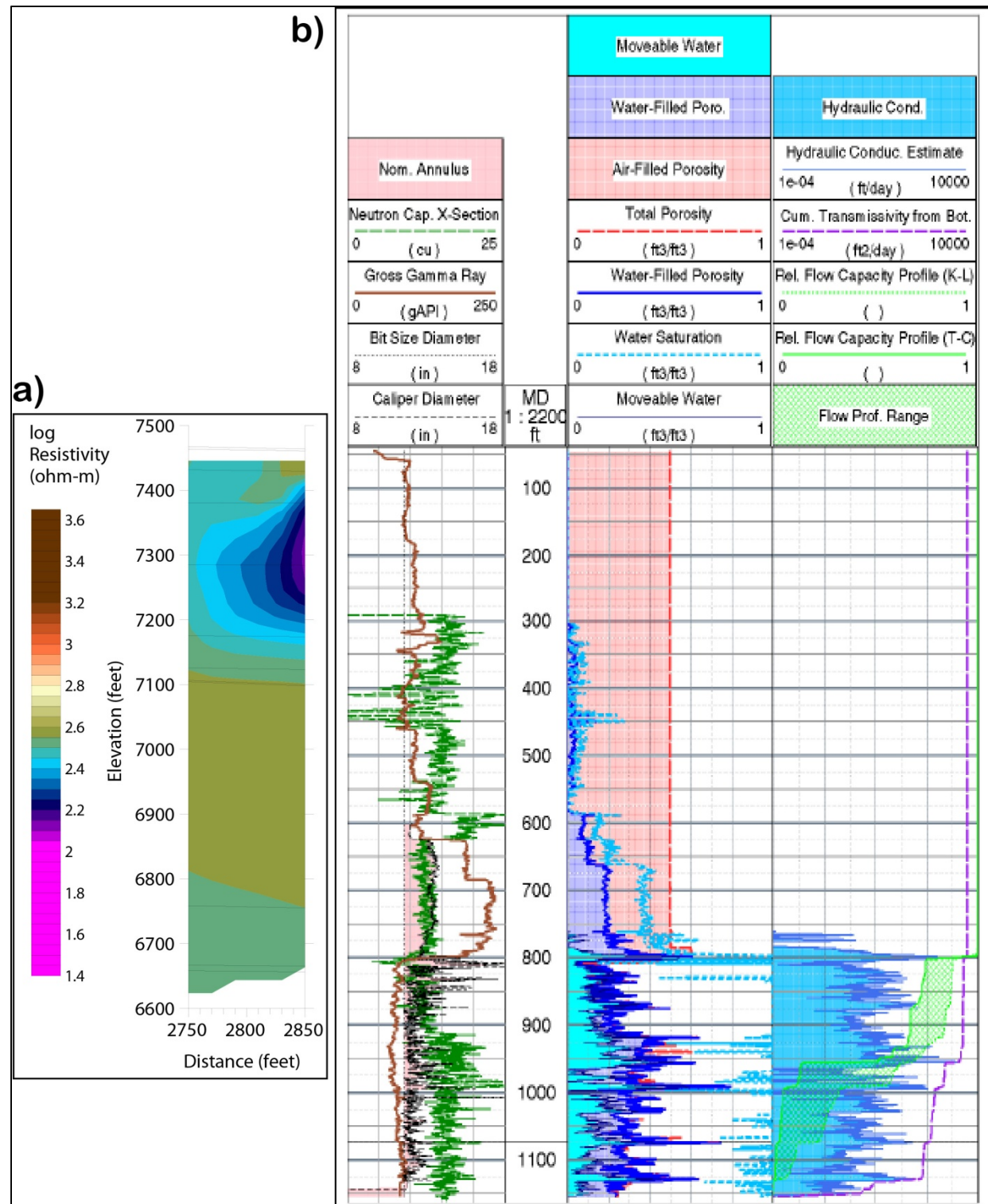
Figure A-4.1-11   Wireline geophysical log of CdV-16-4ip with Line 6 resistivity: (a) resistivity data, and (b) wireline moisture data
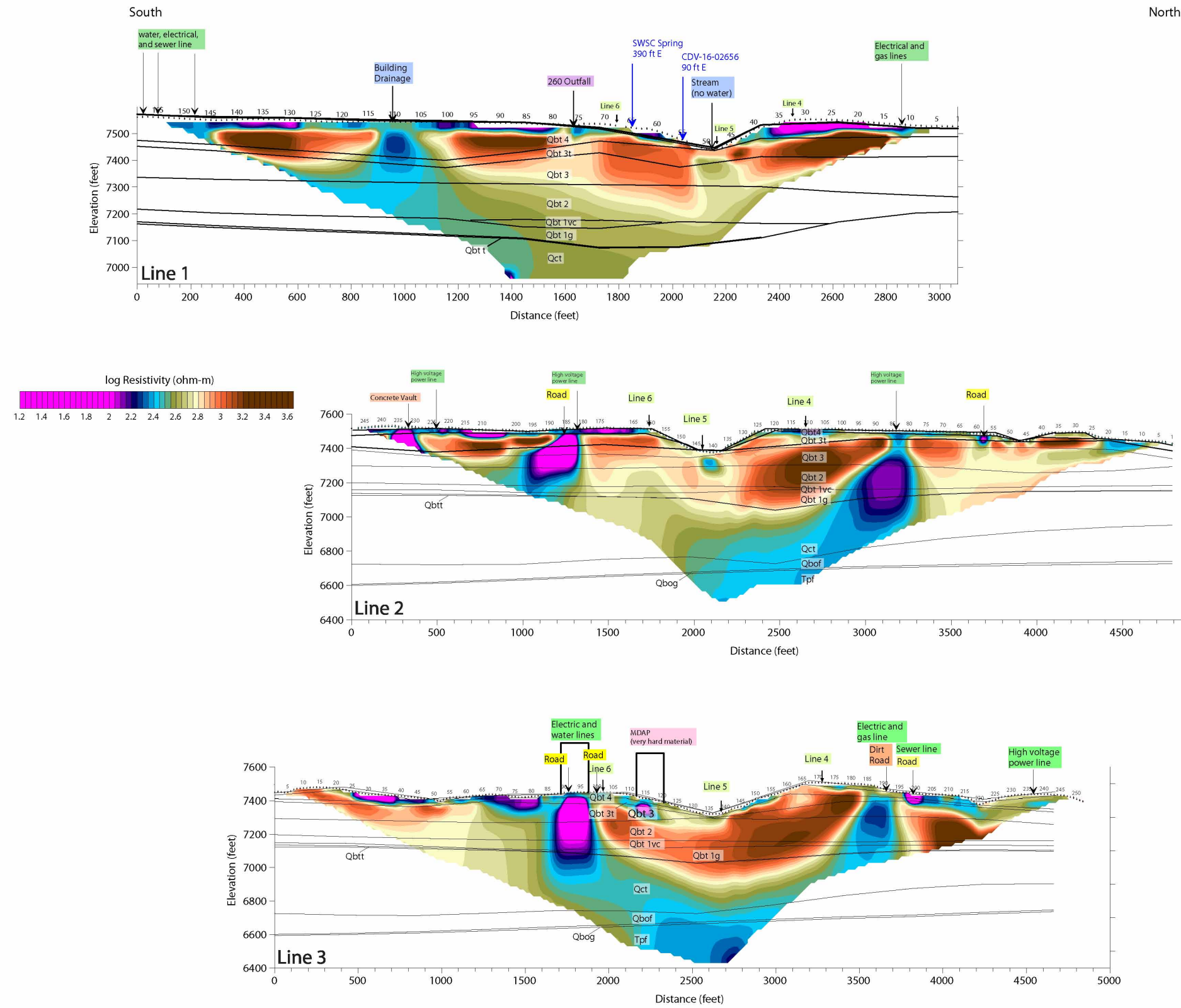
Figure A-4.1-12   Composite of Lines 1 through 3
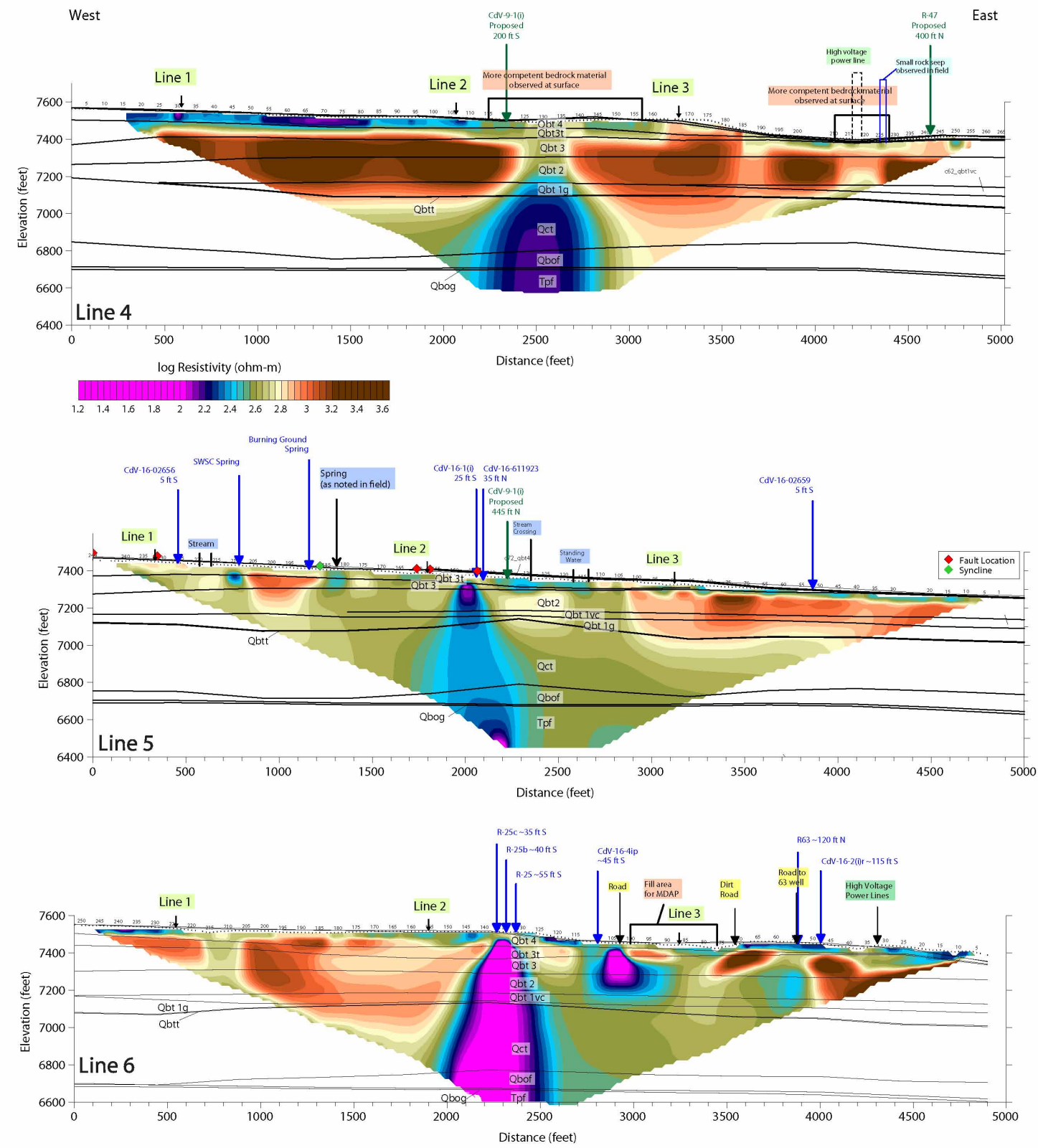
Figure A-4.1-13   Composite of Lines 4 through 6
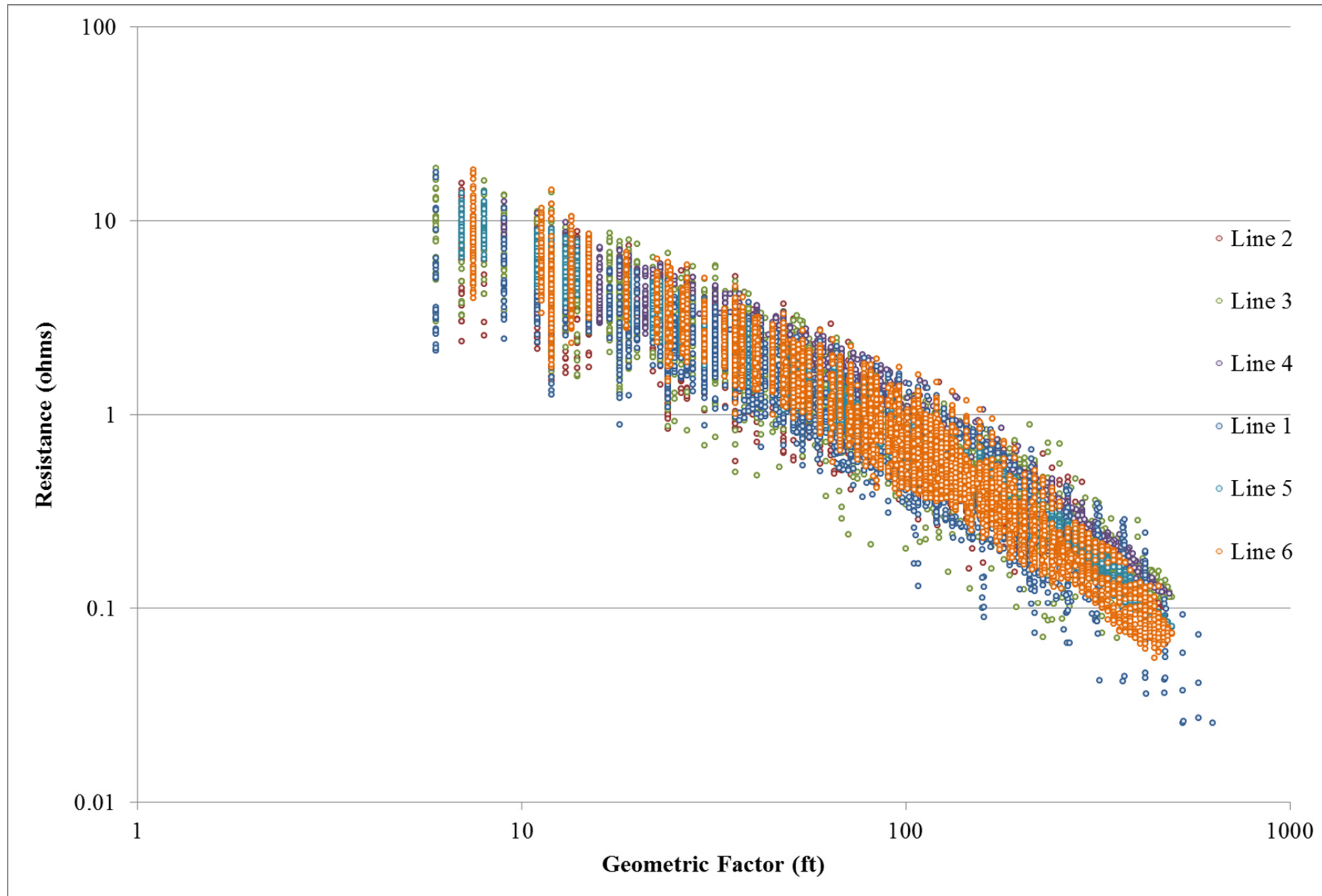
Figure A-4.2-1   Resistance versus geometric factor data for six lines
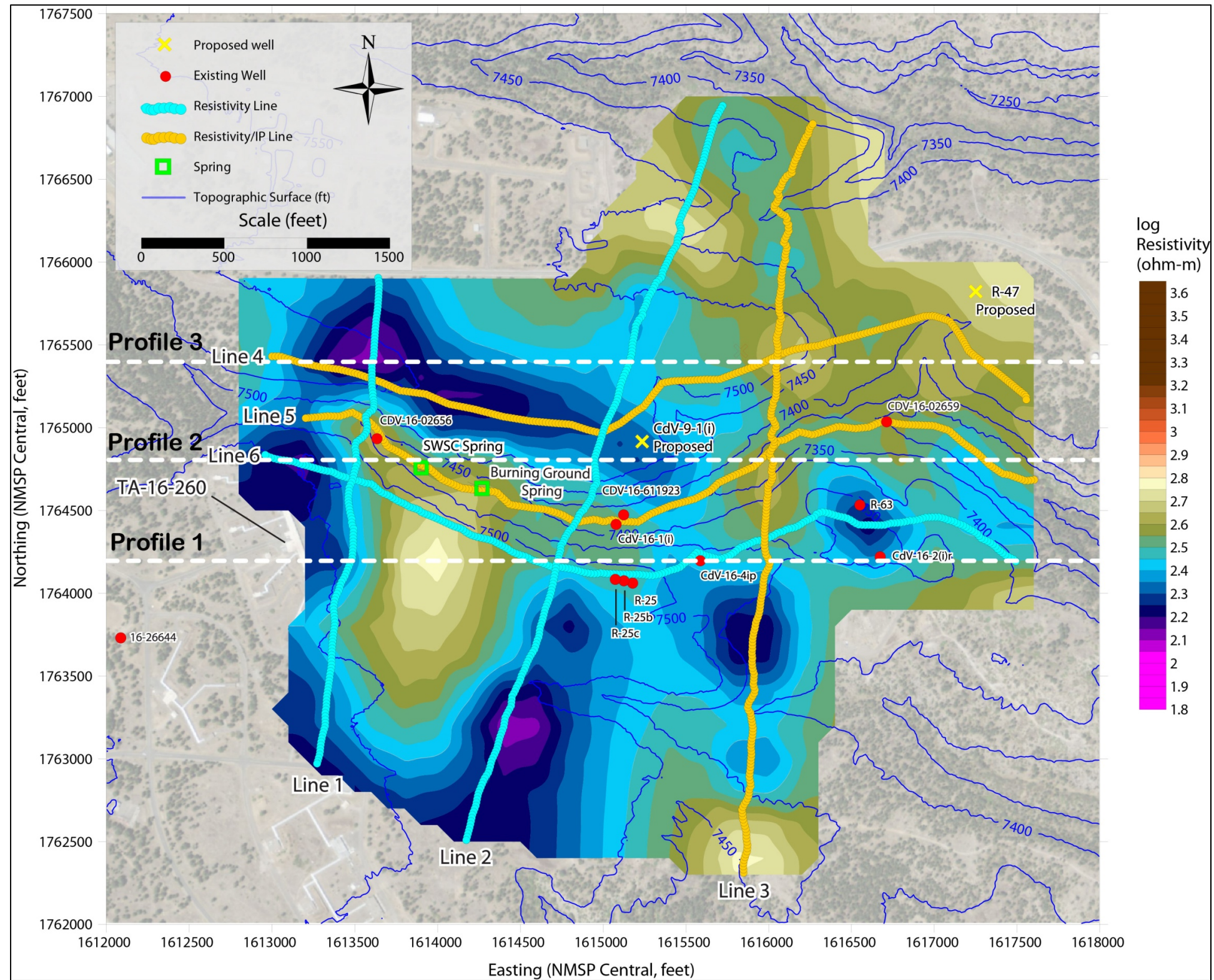
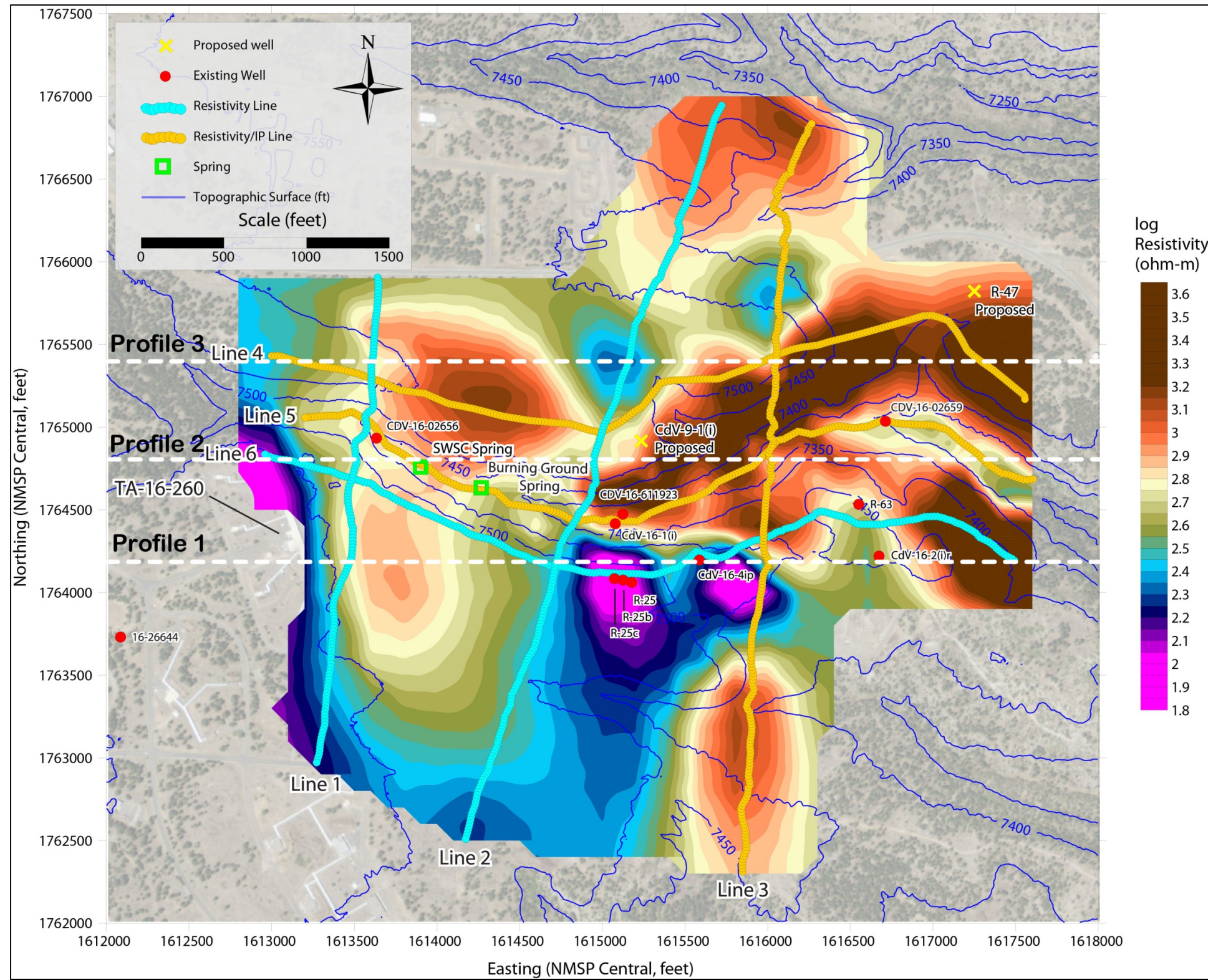**Figure A-4.2-2   Surficial resistivity from the 3-D model of Trial 1**

Figure A-4.2-3 Qbt 2 of the Tshirege Member (elevation 7250 ft) resistivity from the 3-D model of Trial 1
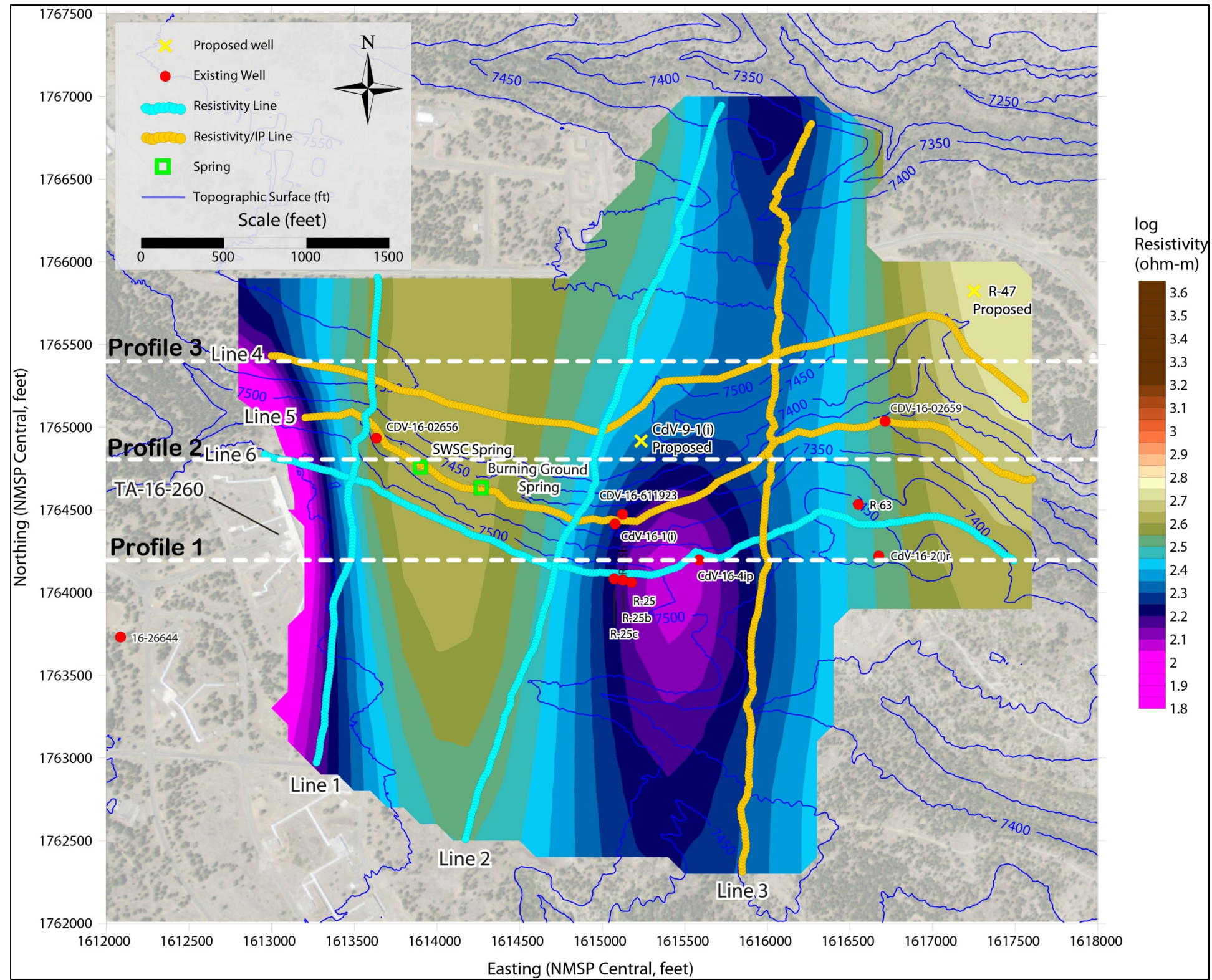
Figure A-4.2-4   Tpf Puye Formation (elevation 6550 ft) resistivity from the 3-D model of Trial 1
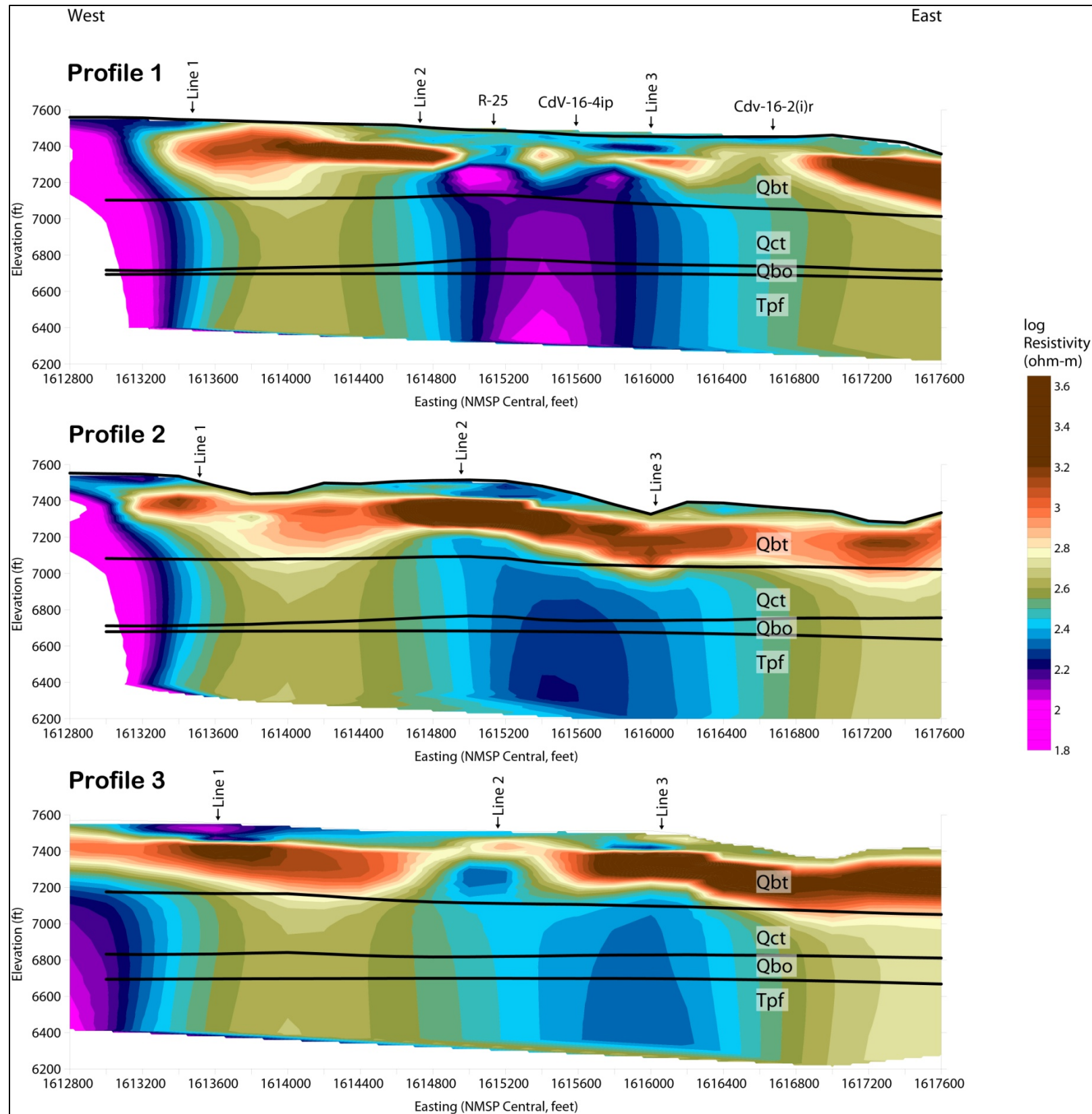
Figure A-4.2-5   Resistivity profiles from the 3-D model of Trial 1
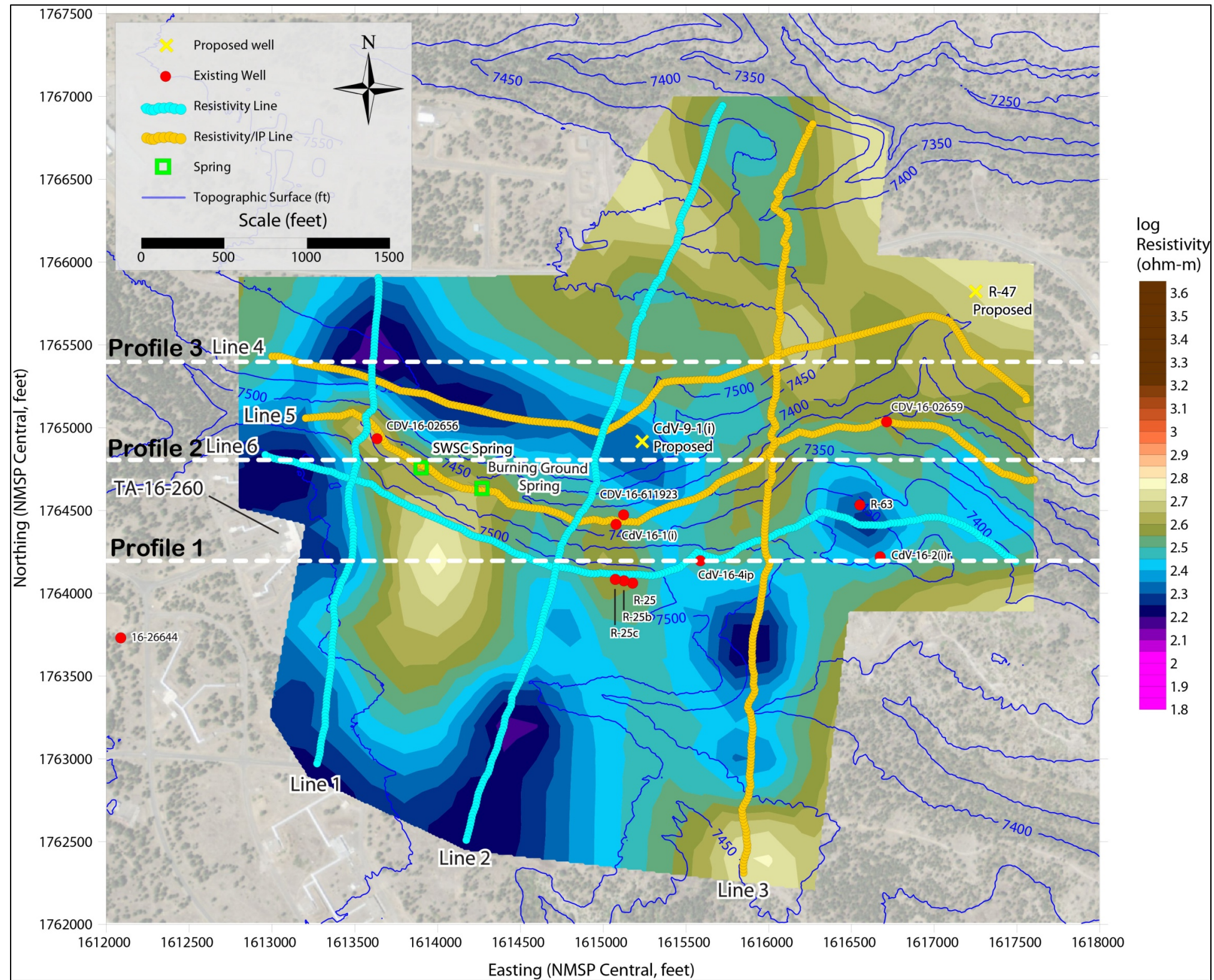
Figure A-4.2-6   Surficial resistivity from the 3-D model of Trial 2
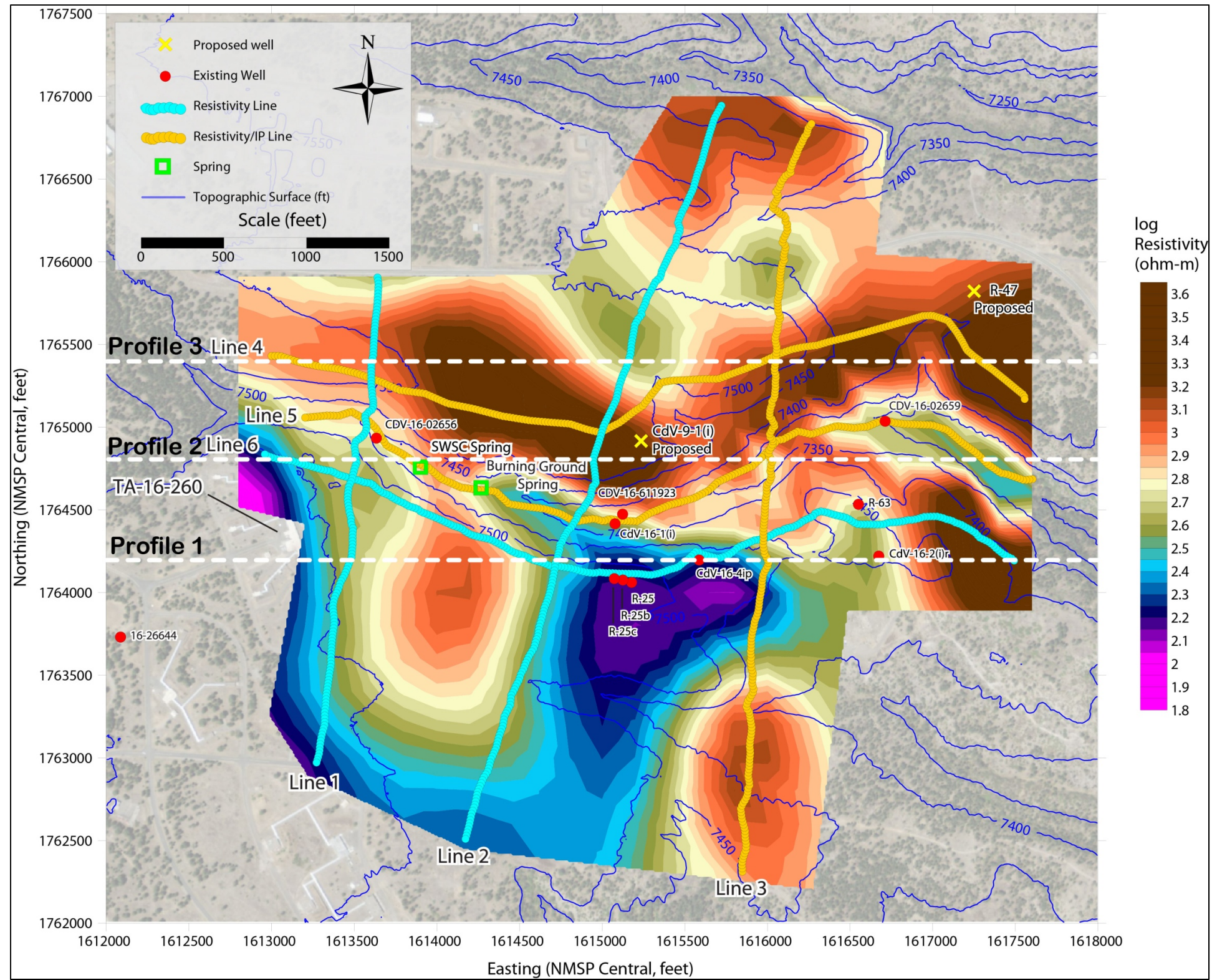
Figure A-4.2-7   Qbt 2 of the Tshirege Member (elevation 7250 ft) resistivity from the 3-D model of Trial 2
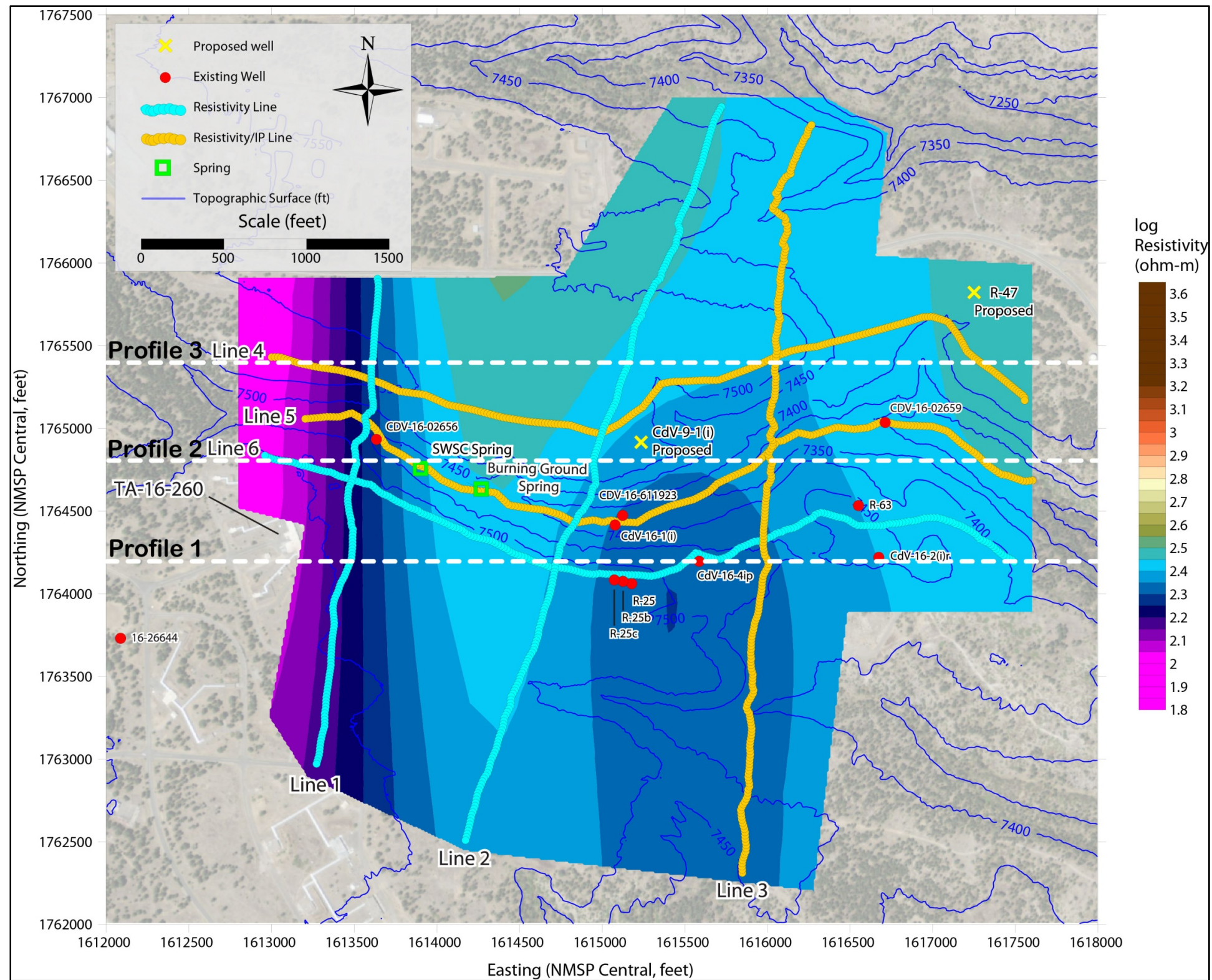
Figure A-4.2-8 **Tpf Puye Formation (elevation 6550 ft) resistivity from the 3-D model of Trial 2**
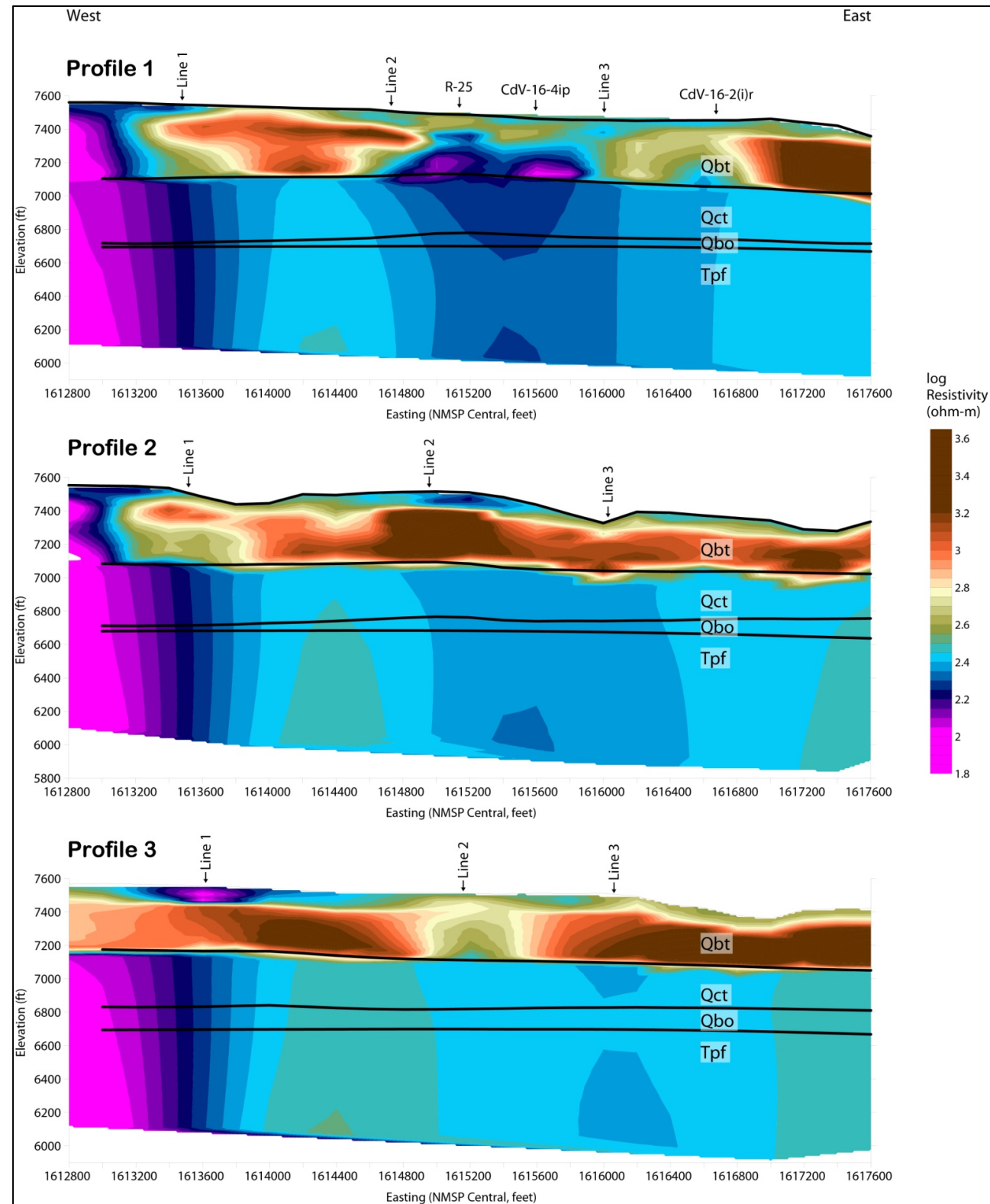
Figure A-4.2-9   Resistivity profiles from the 3-D model of Trial 2

Table A-3.1-1
Geographic Line Details for the Geophysical Survey in CdV

Line Name	Length (ft)	Electrode Quantity	Collection Orientation	Electrode Spacing (ft)	Start Location Easting (NMSP Central, Feet)	Start Location Northing (NMSP Central, Feet)	End Location Easting (NMSP Central, Feet)	End Location Northing (NMSP Central, Feet)
Line 1	3110	159	N-S	20	1613643	1765902	1613276	1762974
Line 2	4882	252	N-S	20	1615725	1766942	1614172	1762501
Line 3	4941	252	S-N	20	1615849	1762317	1616254	1766828
Line 4	5033	266	W-E	16.5, 20[a], 40[b]	1613005	1765433	1617552	1765168
Line 5	4941	252	E-W	20	1617639	1764692	1613215	1765056
Line 6	4941	252	E-W	20	1617484	1764200	1612971	1764833

[a] Schlumberger array.
[b] Wenner array.

Table A-4.1-1
Data Statistics of 2-D Resistivity Profiles

Profile Number	Raw Data Count	Edited Data Count	Minimum	Maximum	Mean
1	3584	3255	80	981	407
2	6632	6176	112	1173	450
3	9413	6908	101	1190	462
4	1723	1662	184	1086	516
5	6797	6442	238	762	456
6	6940	6533	132	1113	429

Measured Apparent Resistivity (ohm-m) spans Minimum, Maximum, Mean.

Appendix B

Electrical Resistivity Survey Data
(on CD included with this document)